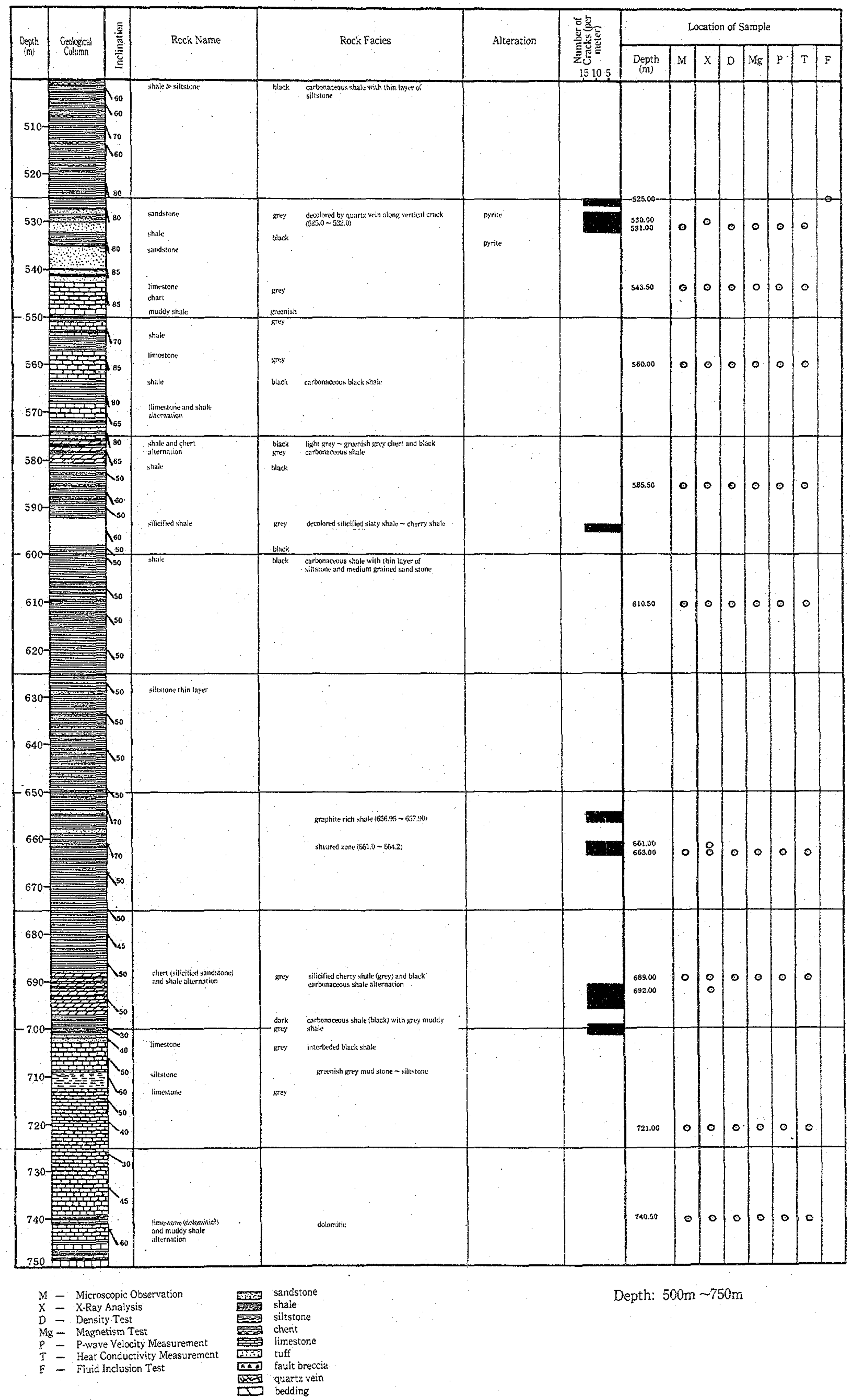

Fig. 3.3-3 Compiled Column of GTE-7 (3)

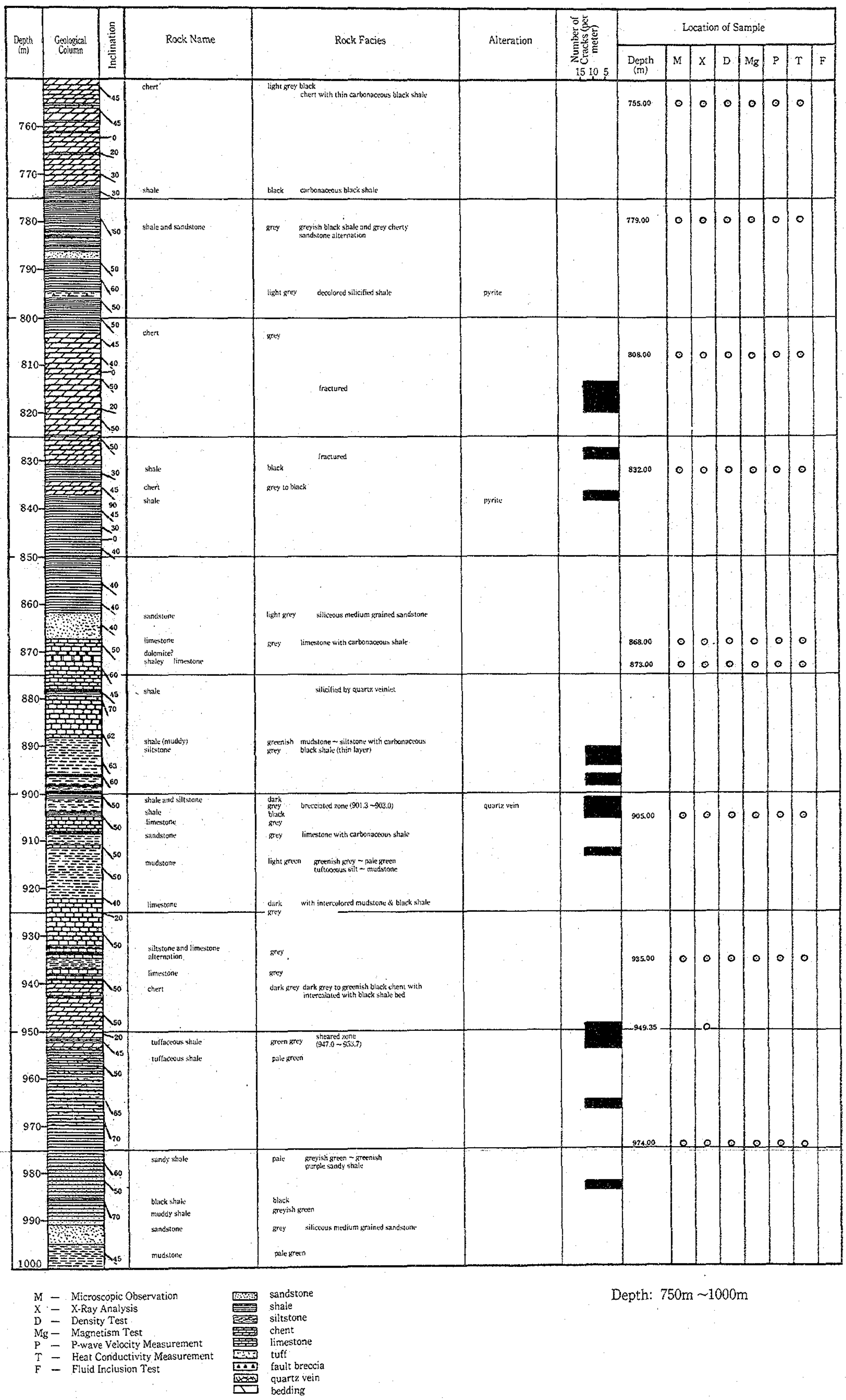

Depth: 750m ~1000m

Fig. 3.3-4 Compiled Column of GTE-7 (4)

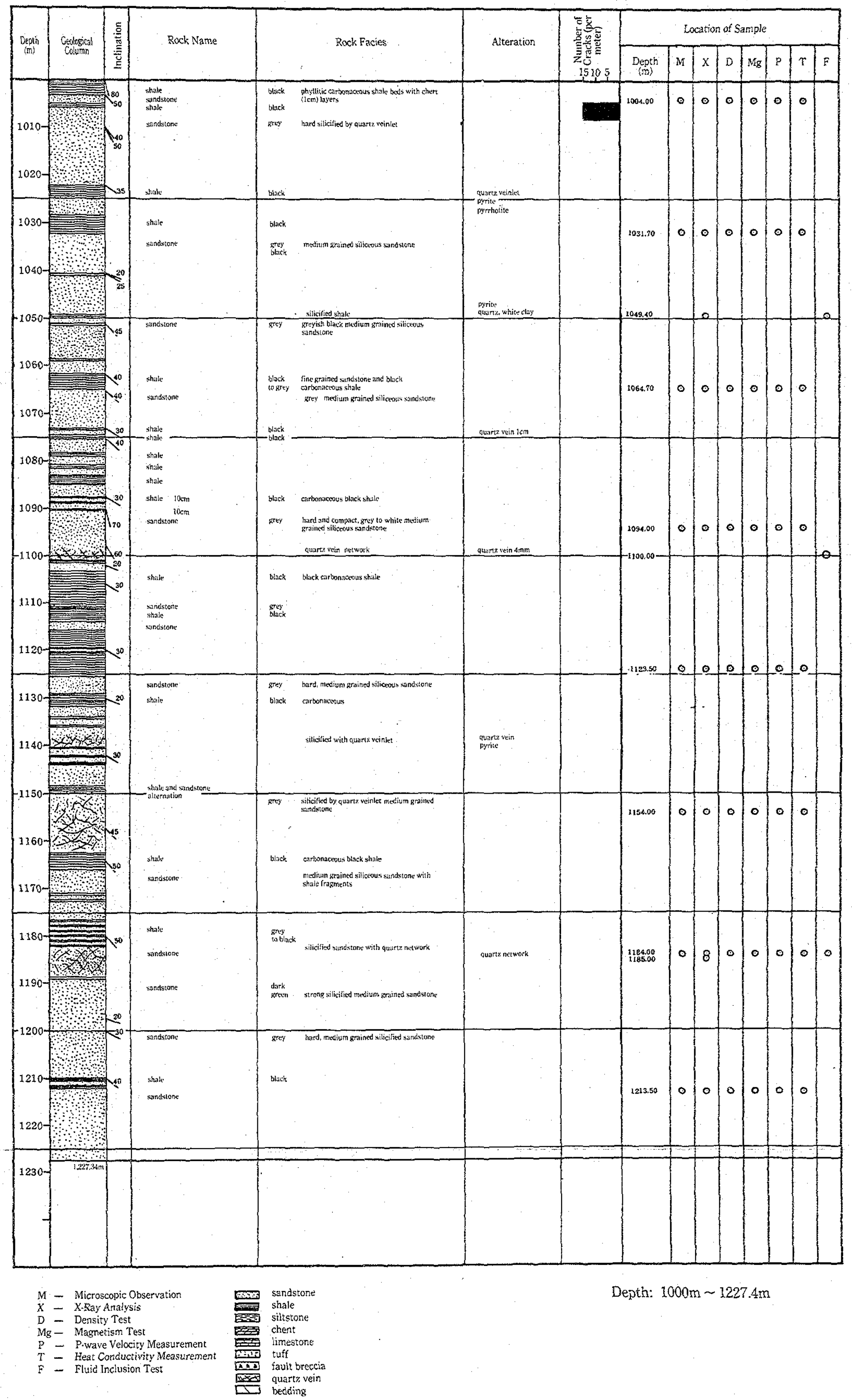

Fig. 3.3-5 Compiled Column of GTE-7 (5)

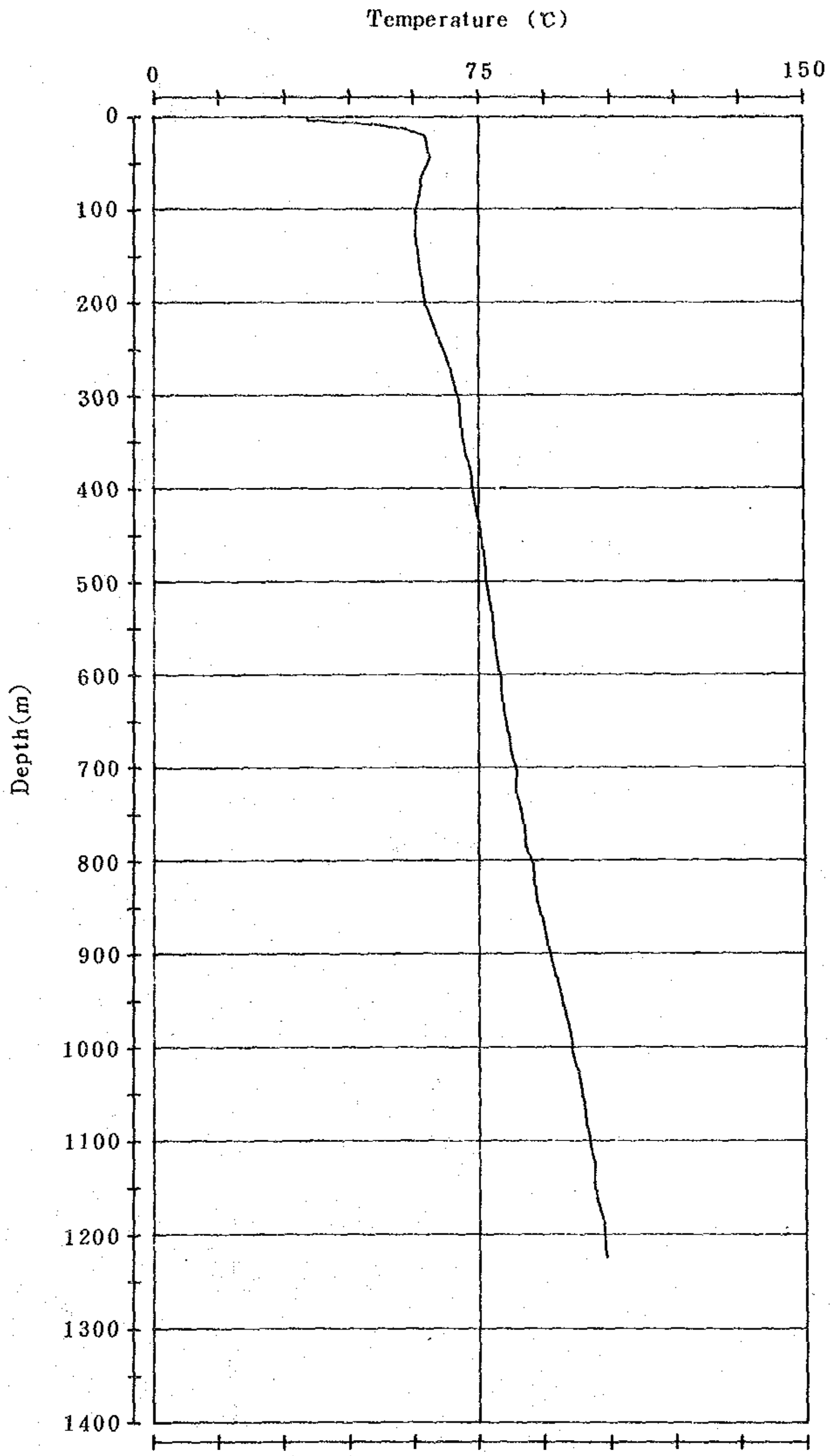

Fig. 3.5-4 Temperature Logging Chart of GTE-7

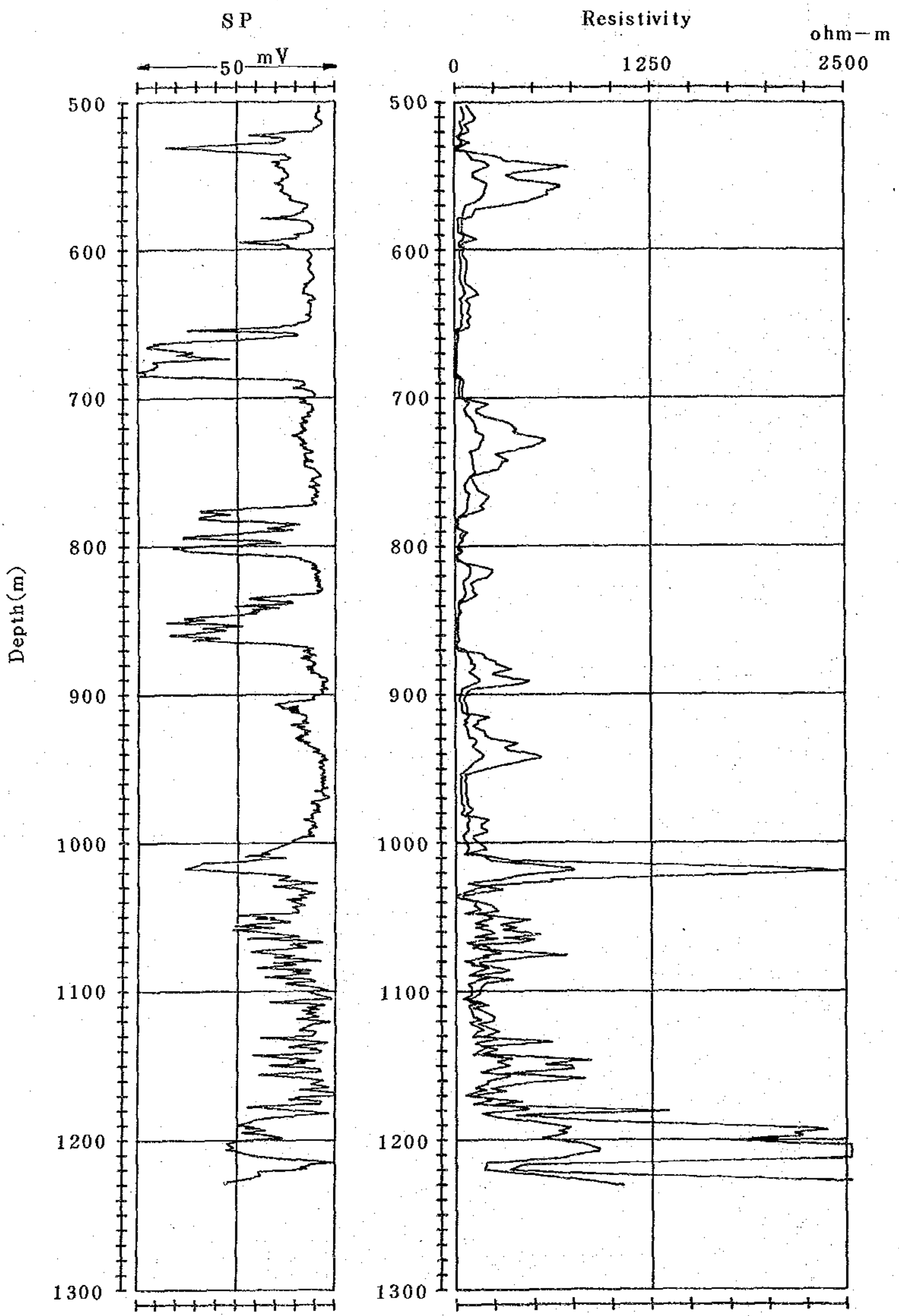

Fig. 3.5-5 Electrical Logging Chart of GTE-7

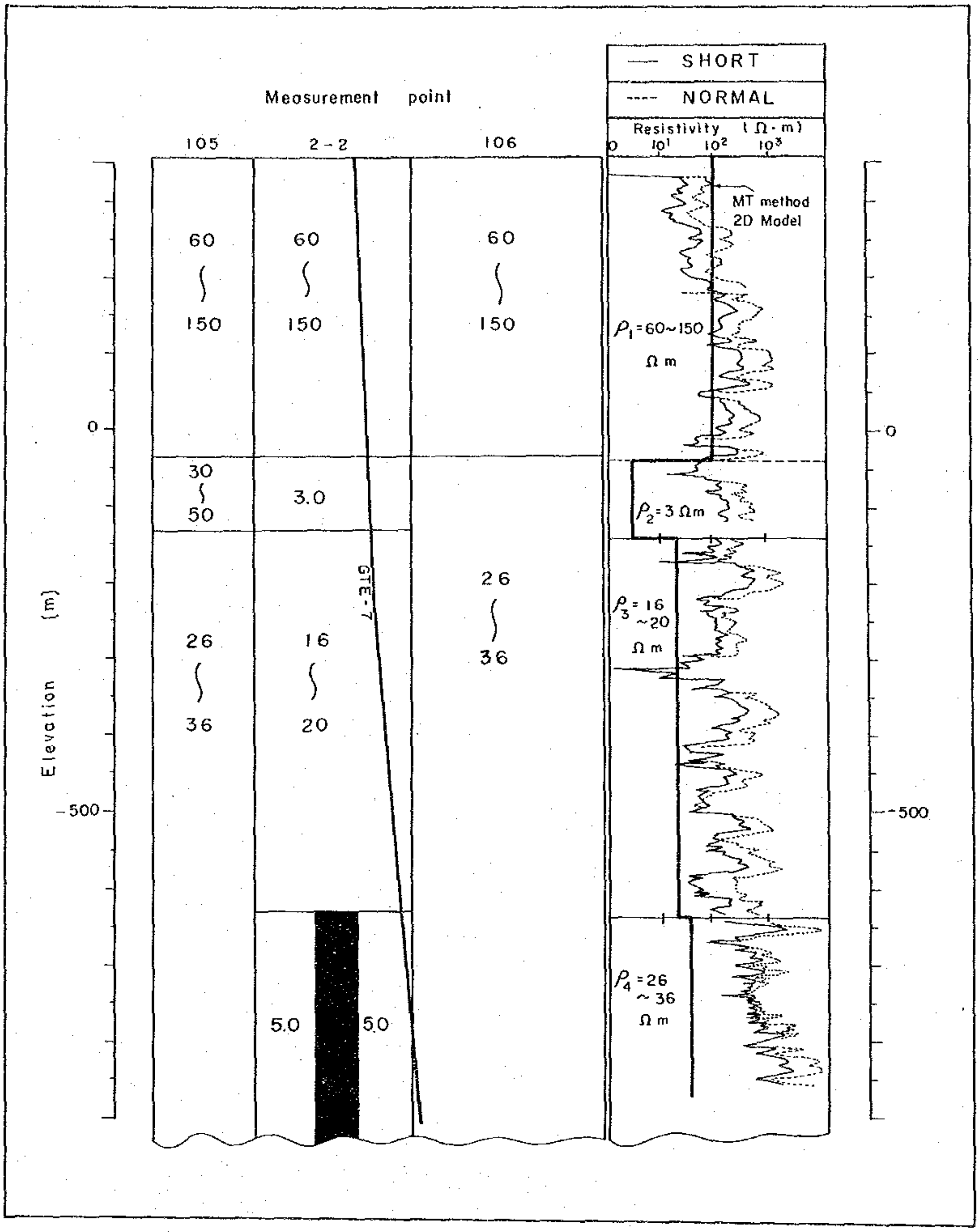

Fig. 3.6-1 Comparison of MT Interpretation Result and Electrical Well Logging Result (GTE-7)

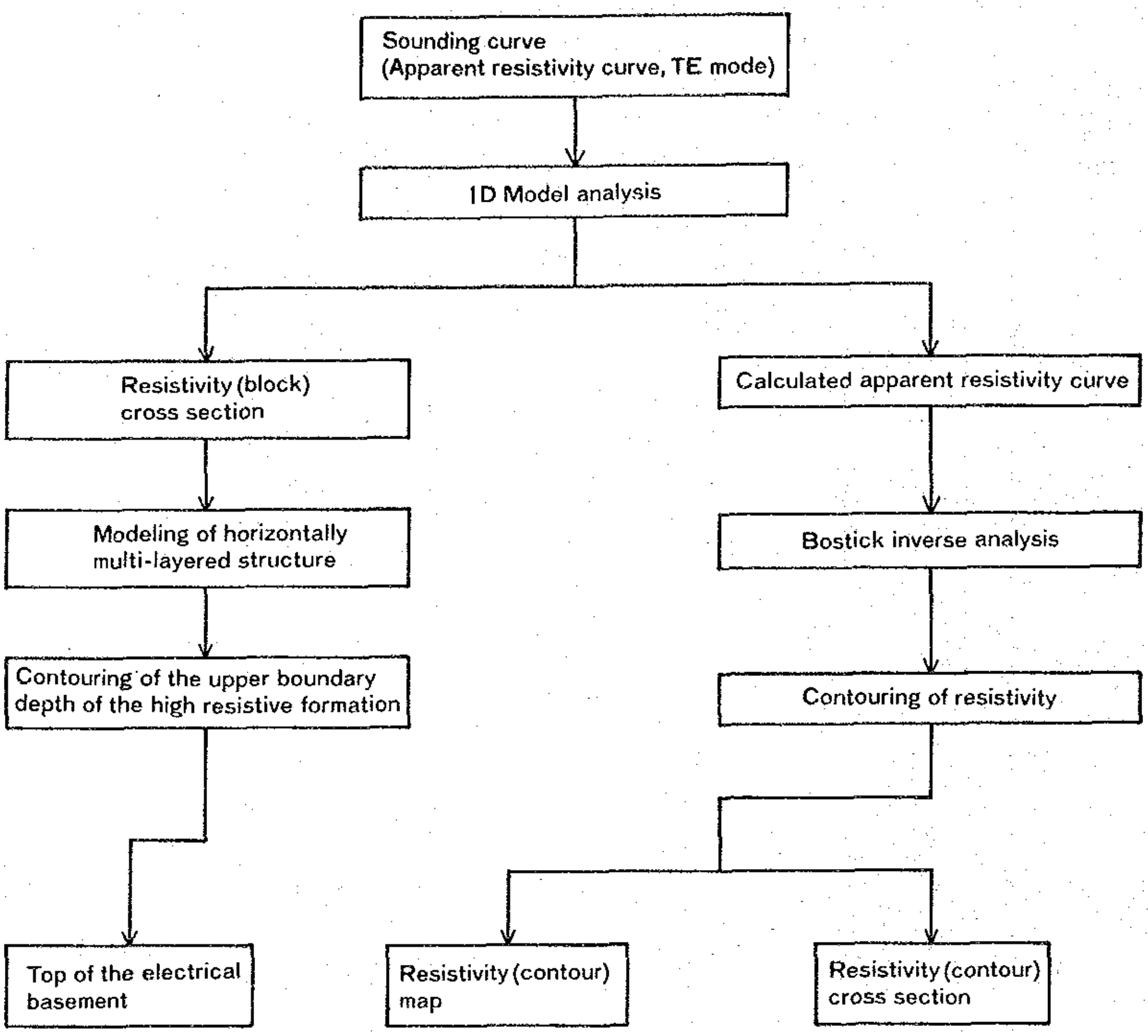

Fig. 3.6-2 Flow Chart of Interpretation (2nd Time)

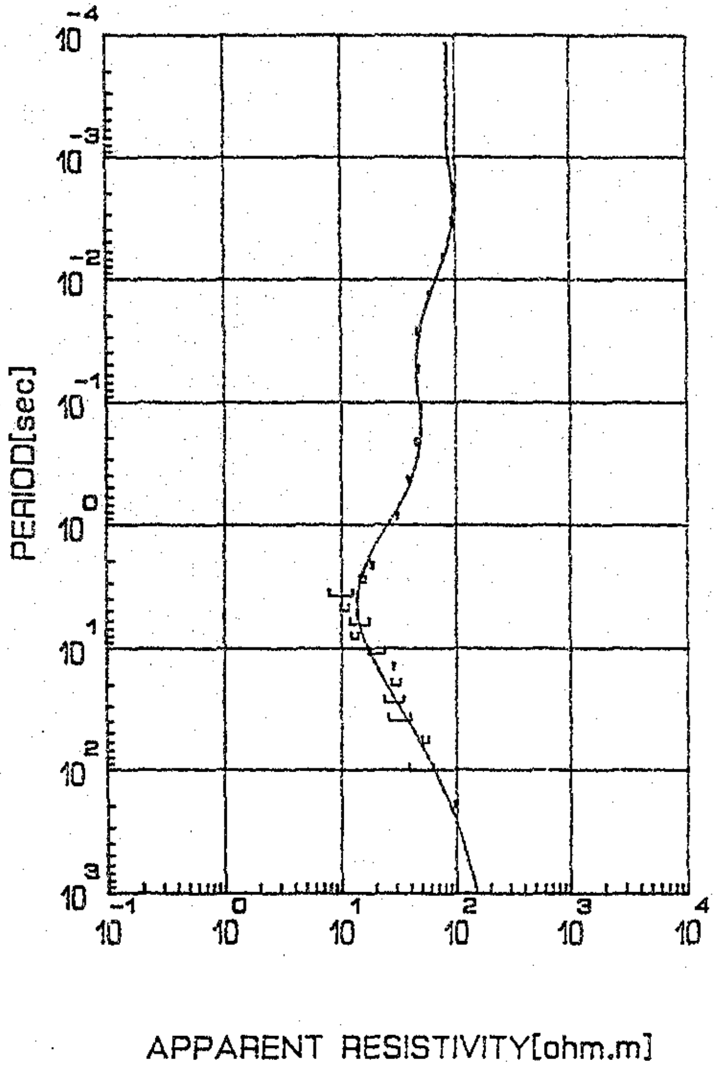

MODEL

(ρ (Ωm))	(h (m))
86.03	310.3
4.900	28.96
49.35	1189.
5.298	1265.
251.1	

OPTIMAL MODEL
Area
SAN KAMPAENG
Stn. 4-5
ELV 410(m)
CORX 4760(m)
CORY 3130(m)
MES.DATE
1983
ANA.DATE
1983
XY
YX

Fig. 3.6-3 Example of 1D Model Inversion

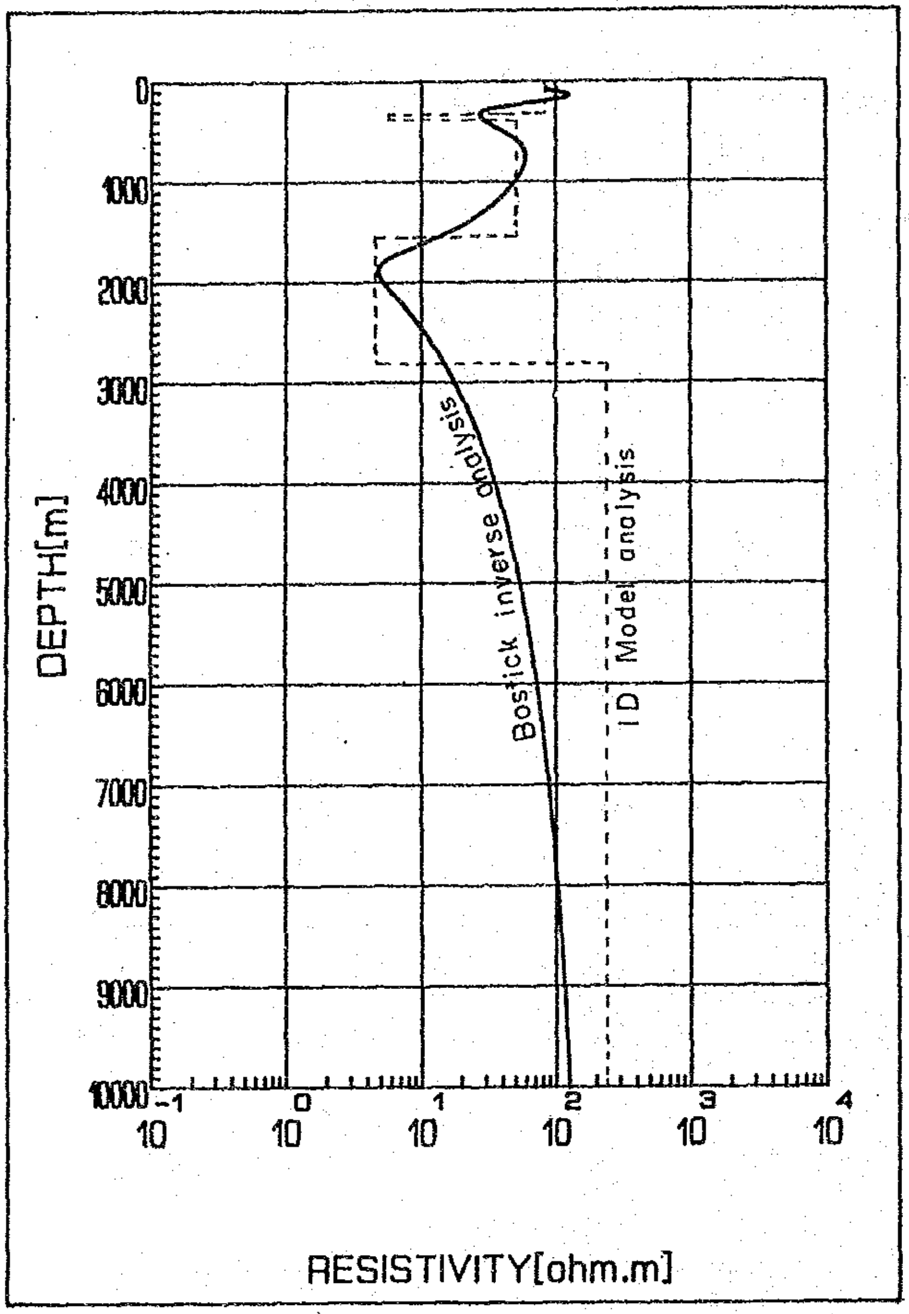

Fig. 3.6-4 Comparison of 1D Model Interpretation and Bostick Inverse Interpretation

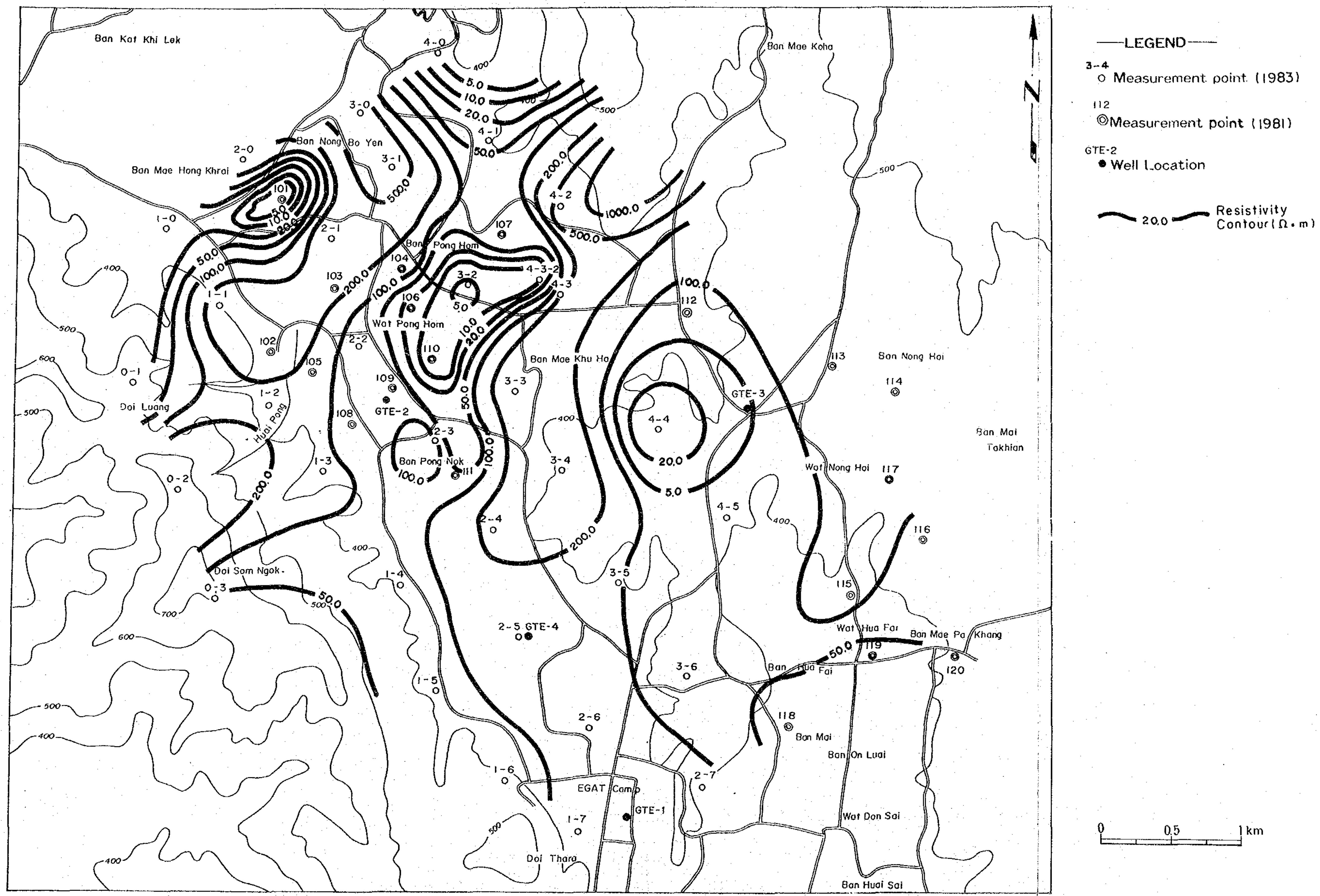

Fig. 3.6-5 Resistivity Map (SL=-200m)

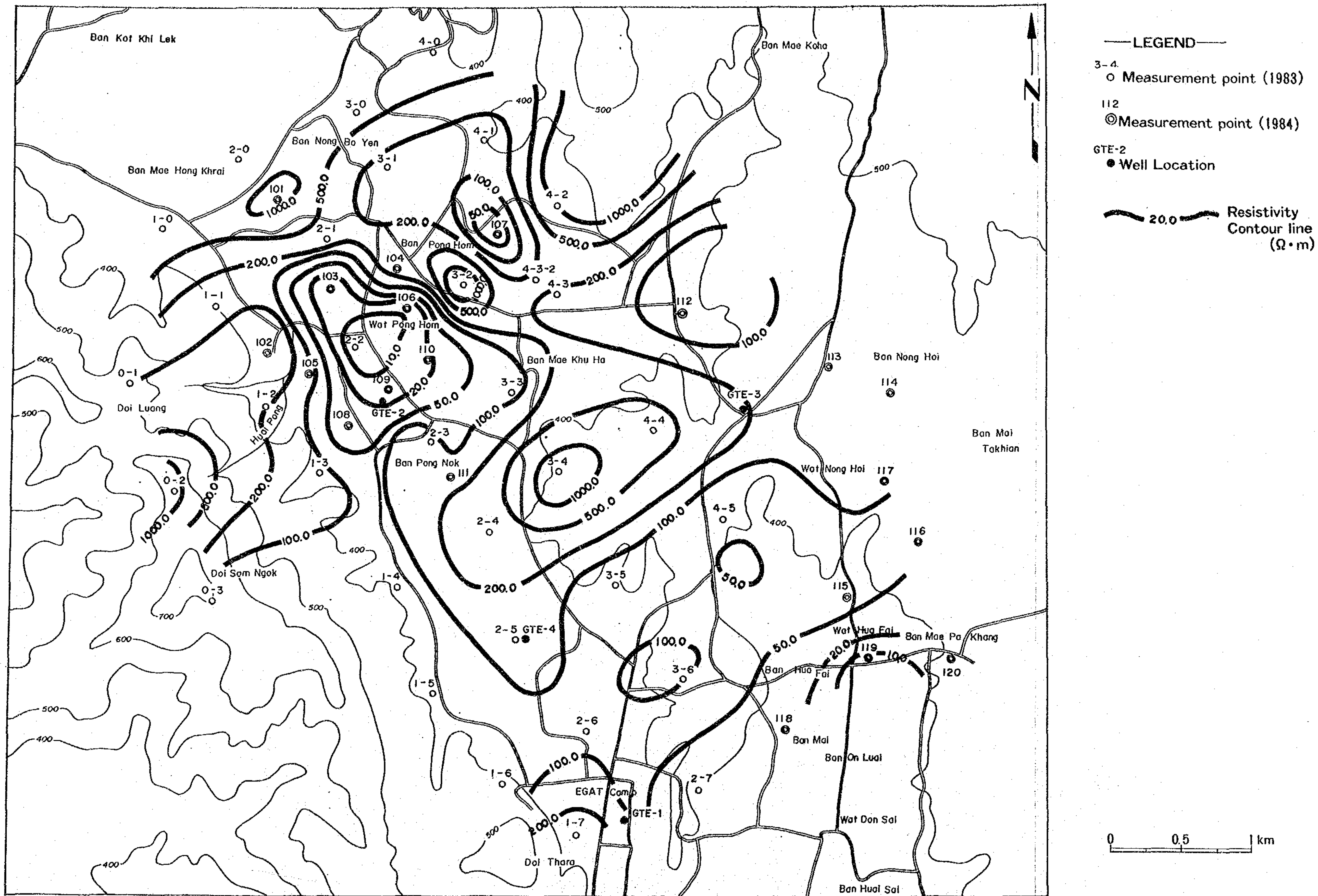

Fig. 3.6-6 Resistivity Map (SL=-500m)

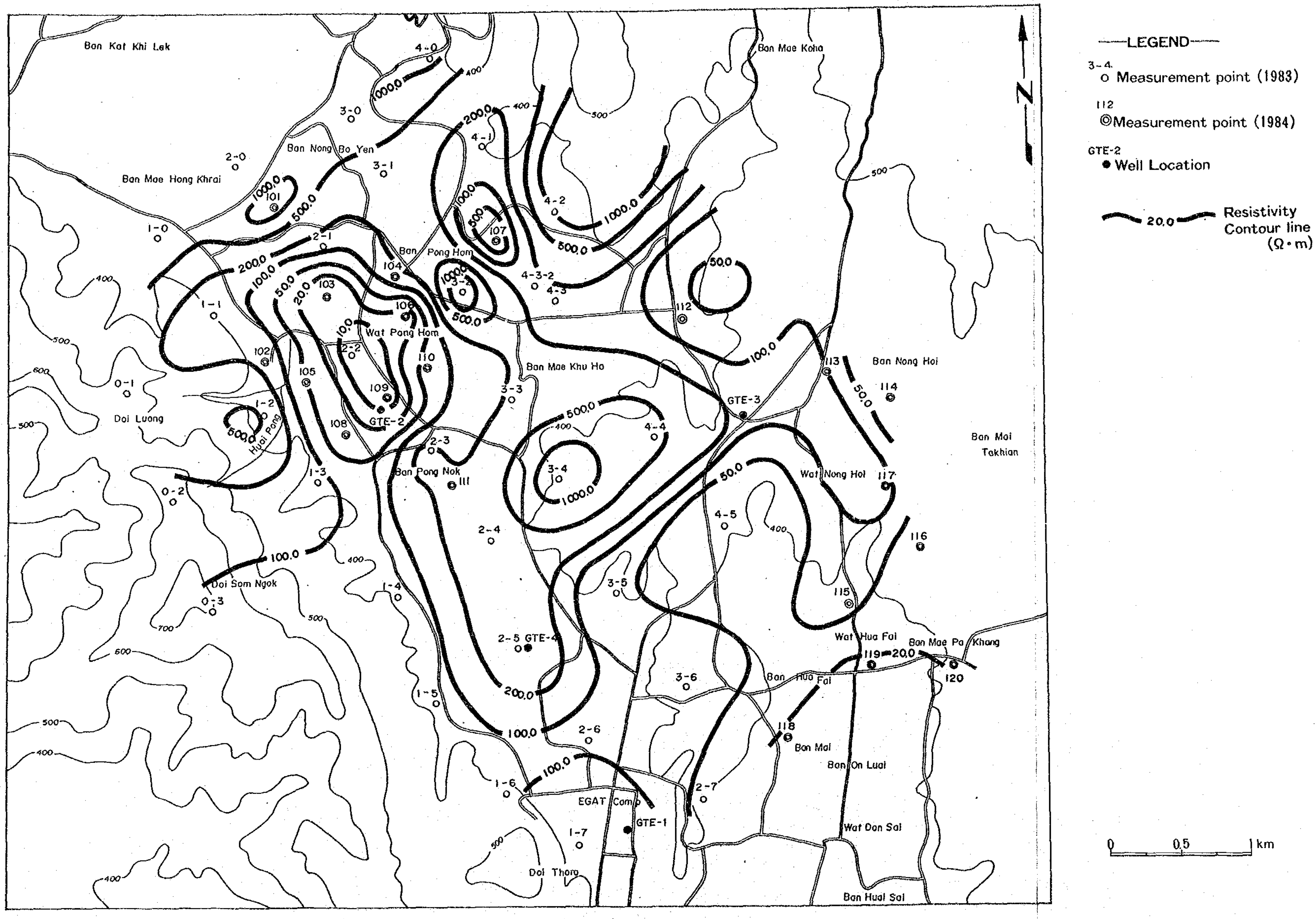

Fig. 3.6-7 Resistivity Map (SL=-1,000m)

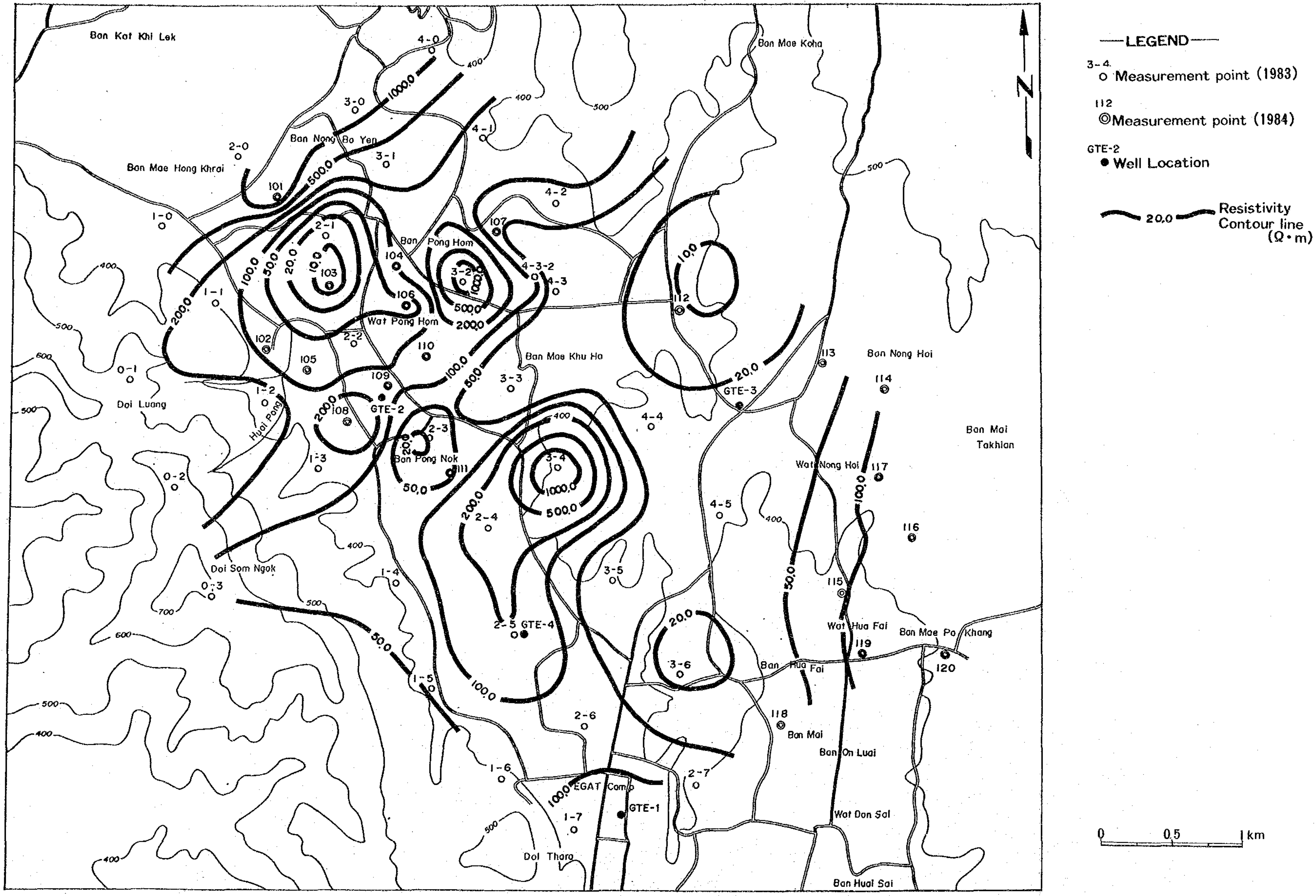

Fig. 3.6-8 Resistivity Map (SL=-3,000m)

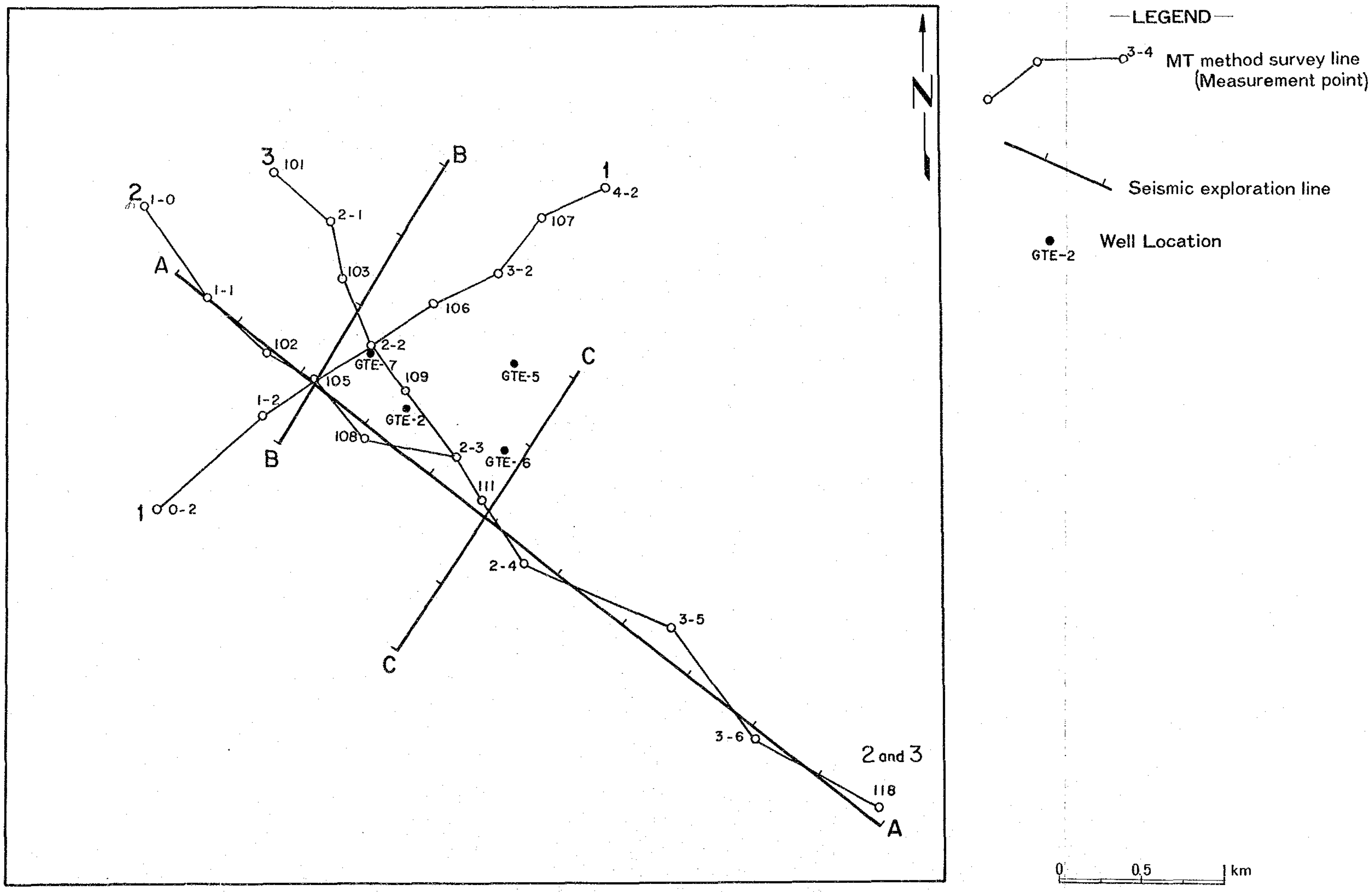

Fig. 3.6-9 Location Map of Cross Section

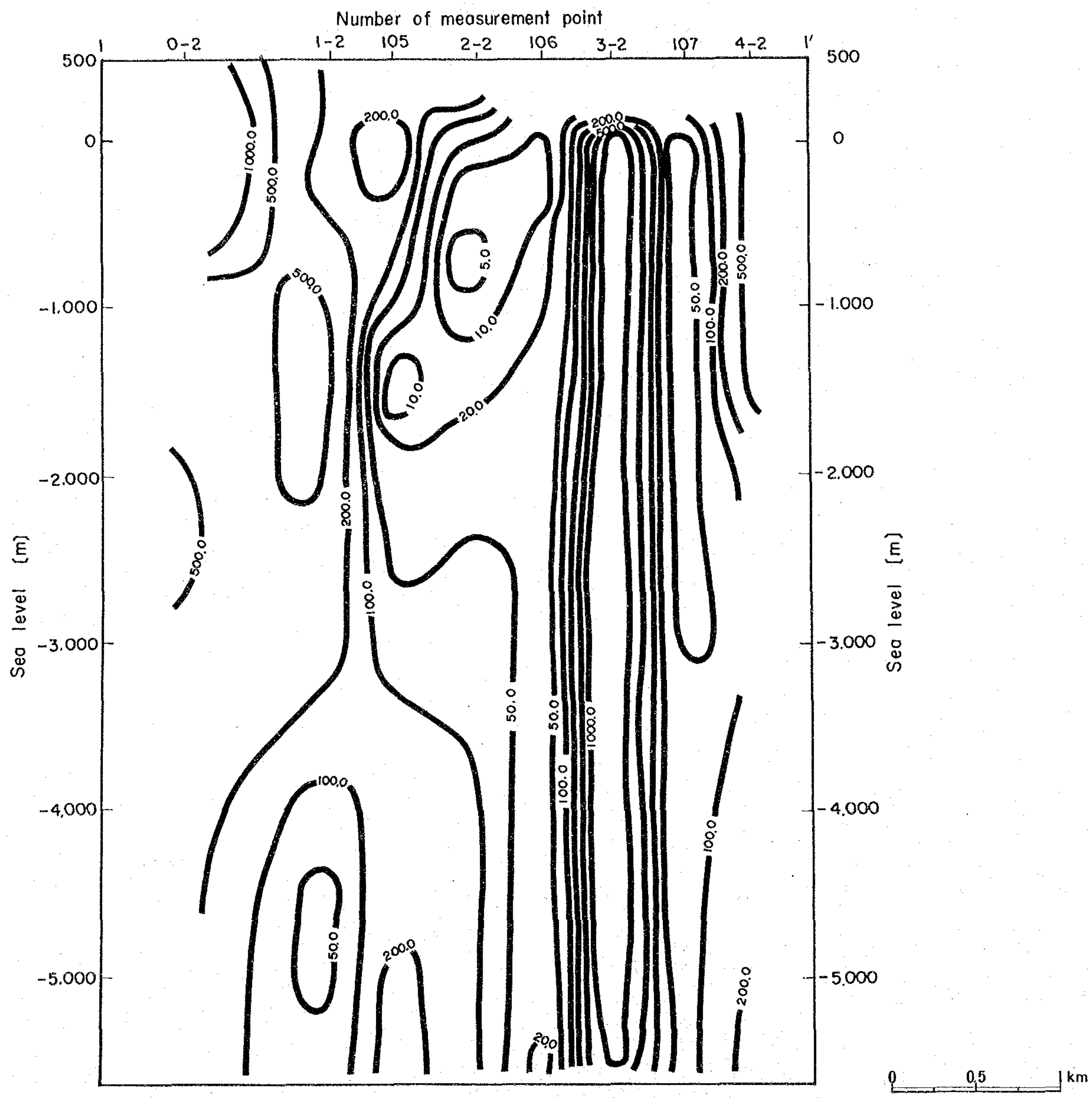

Fig. 3.6-10 Resistivity Cross Section (Line 1)

—LEGEND—

20.0 Iso resistivity line (Ω・m)

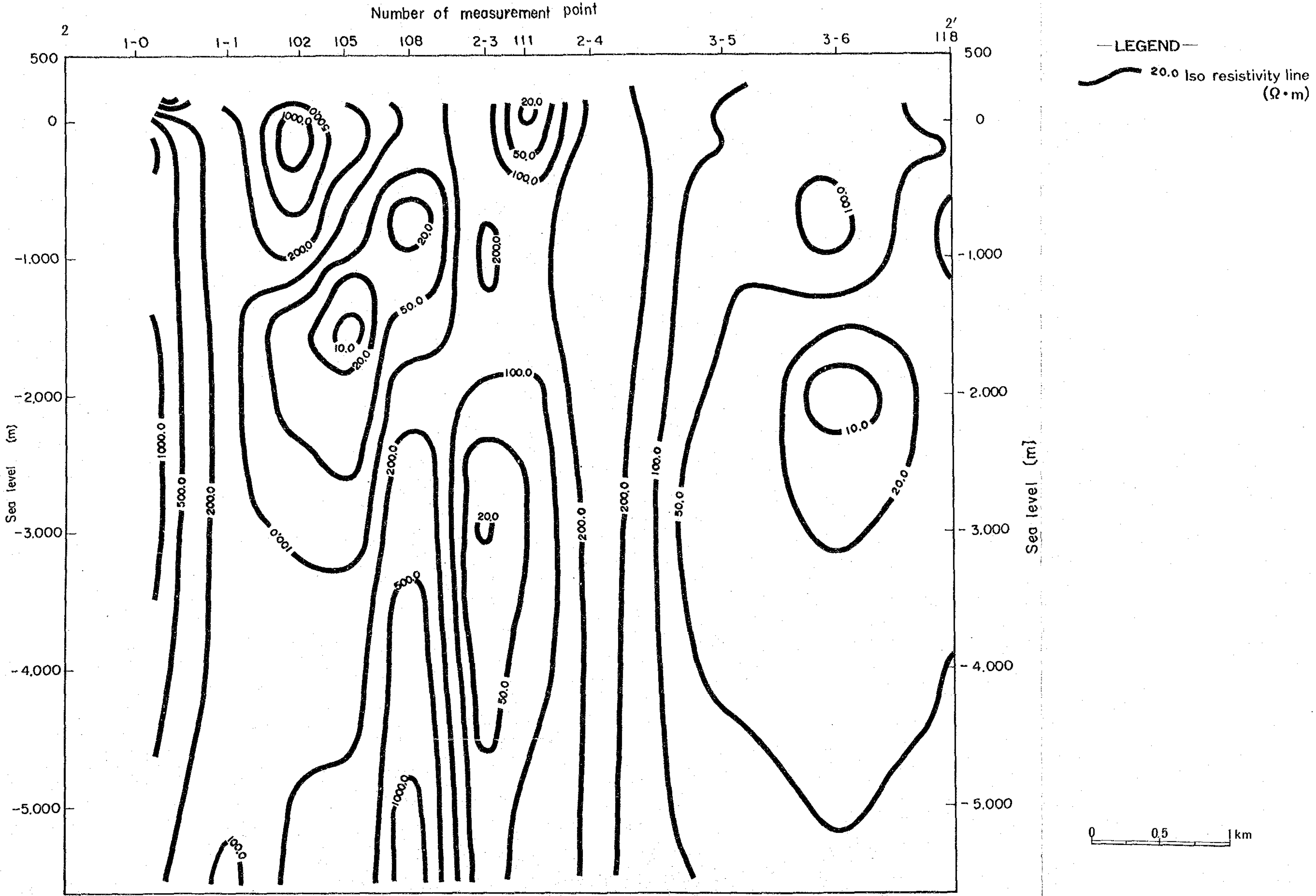

Fig. 3.6-11 Resistivity Cross Section (Line 2)

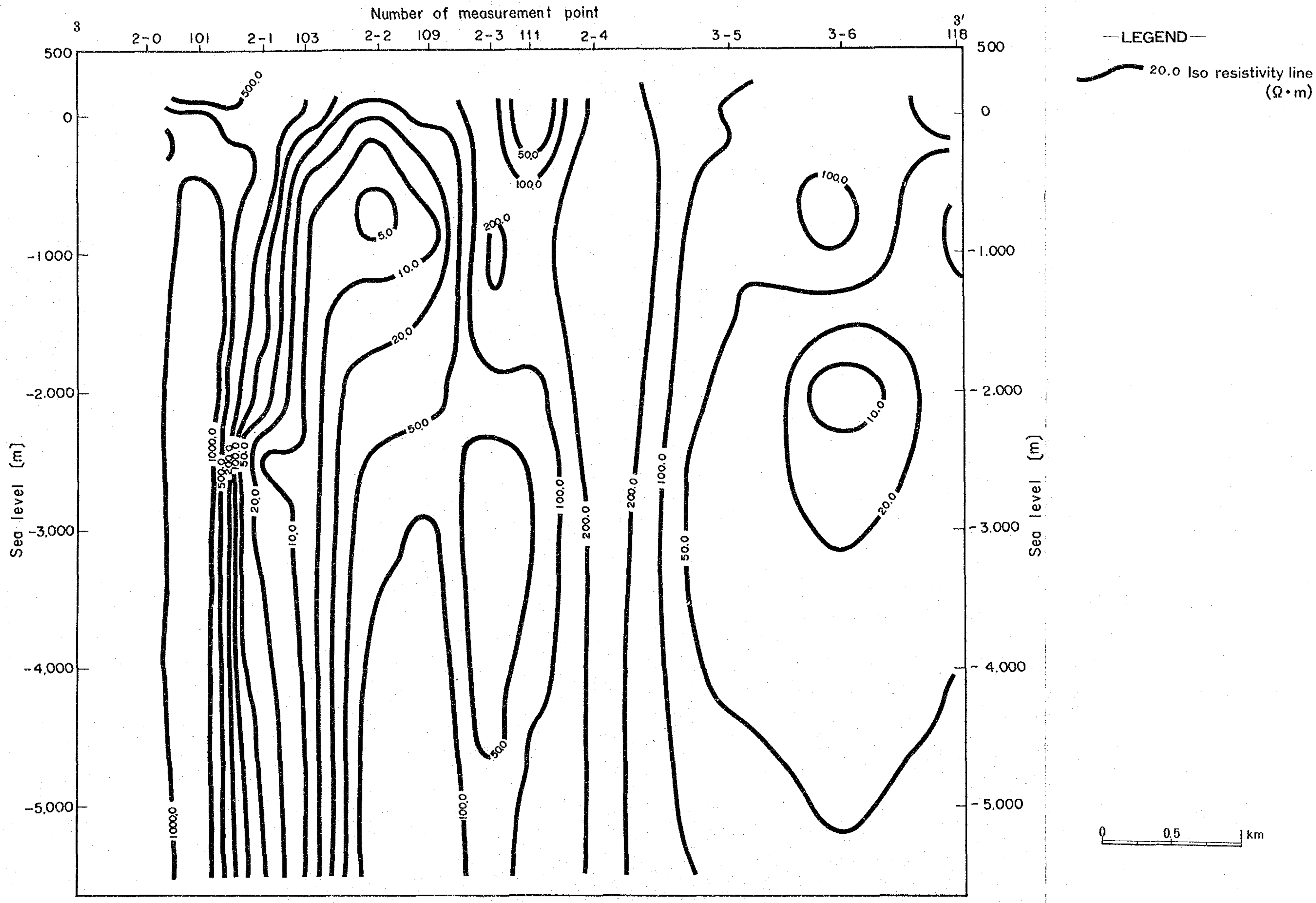

Fig. 3.6-12 Resistivity Cross Section (Line 3)

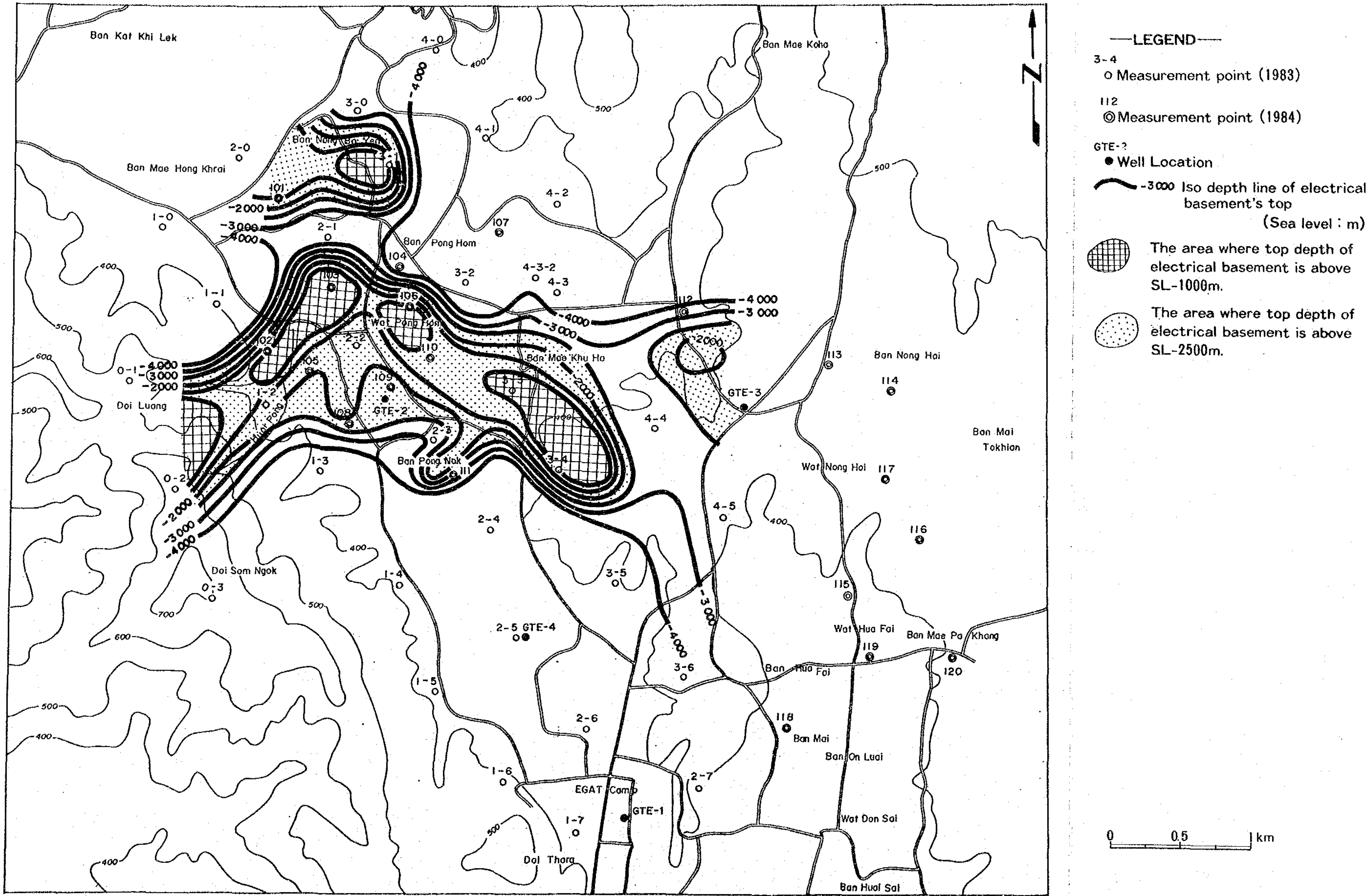

Fig. 3.6-13 Electrical Basement Map

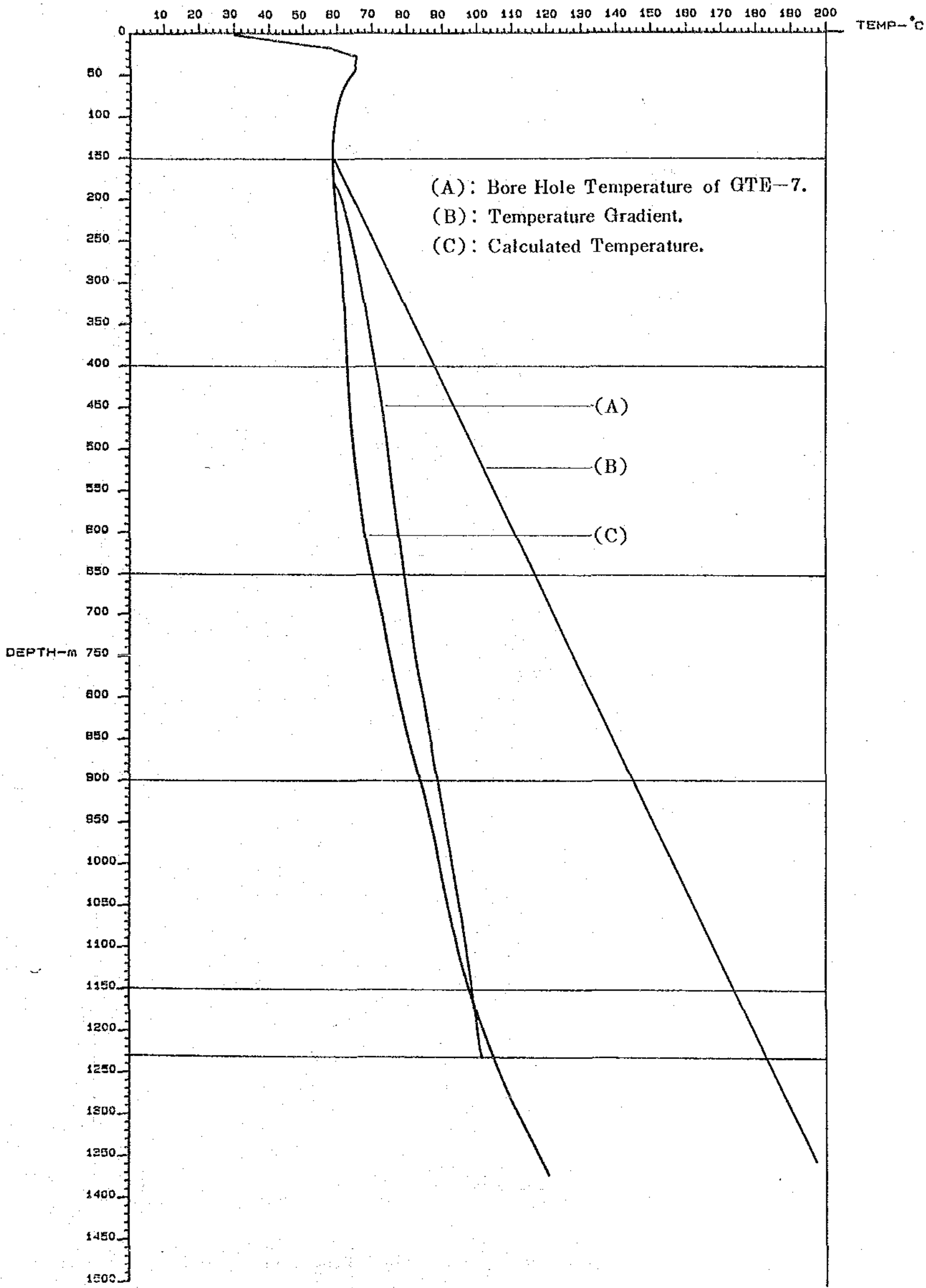

Fig. 3.7-1 Relationship of Depth and Temperature of Penetration Water

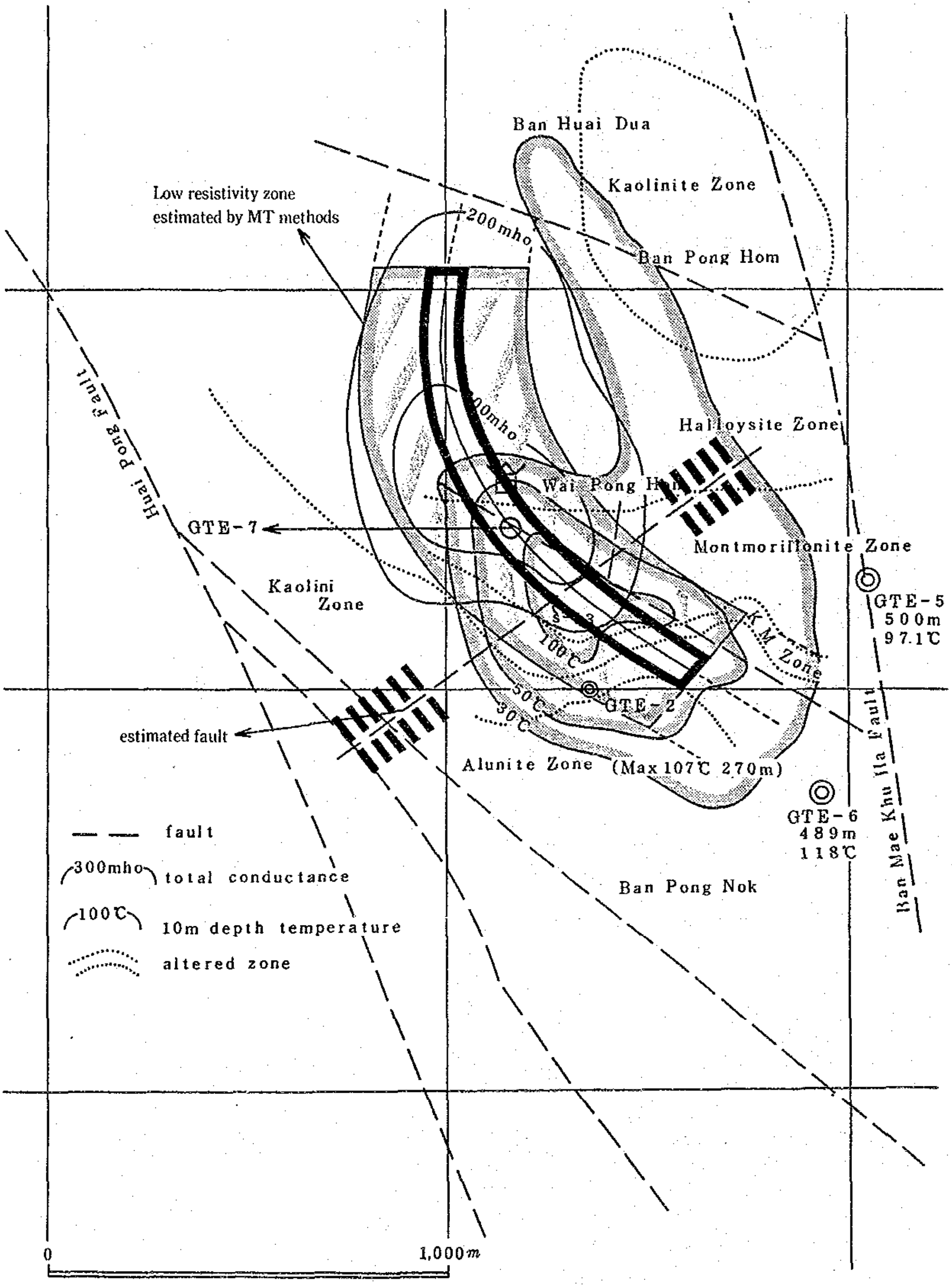

Fig. 3.7-2 Geothermal System Revised by Drilling Data of GTE-7

Table 3.2-1 Summary of Drilling Work of GTE-7

Depth (m)	Well Diameter (mm)	Bit				Drilling mud				Casing		Lithology	Drilling activities
		Type	Size	Bit lord (kg)	Rotation (r.p.m)	Temperature in/out (℃)	Mud Supplied (L/min)	Type	Lost Circu-lation	Size (inch)	Depth inserted (m)		
0.00 ~ 4.20	357.60	S.C.T	357.6	1000	40	–	100	Bentonite	–	14	4.20	Over burden	Penetration rate: 2.75m/h
4.20 ~ 30.00	311.20	Tricone	$12\frac{1}{4}''$	1000 ~3000	45	–	850	Bentonite	80ℓ/min at 1500m	10	28.10	Shale, Sandston	Coring: 13.14m~16.78m Core recovery: 76.6% 10″CP one plug cementation Penetration rate: 1.59m/h
	101.00	Diamond	HQ-WL	500 ~1000	60		100	Bentonite					
30.00 ~ 200.00	244.50	Tricone	9-5/8″	3000 ~5000	40~ 60	40.9/39.5 ~ 47.5/48.2	850	Libonite	None	8″	199.00	Shale Sandstone Siltstone Limestone	Core recovery: 96.5% None core Penetration rate: 1.29m/h 8″CP two plug cementation
	101.00	Diamond	HQ-WL	1000	70		150						
200.00 ~ 504.00	193.70	Tricone	7-5/8″	1000 ~4000	40~ 45	47.7/48.0 ~ 37.2/45.5	600~700	Libonite	30ℓ/min at 455.00m	6″	501.00	Shale Limestone Chart Sandstone Siltstone	Core recovery: 97.1% None core Penetration rate: 0.96m/h 6″CP two plug cementation
	101.00	Diamond	HQ-WL	700 ~1500	100~120		100~150						
504.00 ~1002.75	142.90	Tricone	7-5/8″	1000 ~3000	40~ 50	34.3/44.2 ~ 36.3/43.9	350	BH	None	$4\frac{1}{2}''$	1000.00	Shale Limestone Chart Sandstone Siltstone	Core recovery: 99.6% None core Penetration rate: 1.35m/h $4\frac{1}{2}''$ CP one plug cementation
	101.00	Diamond	HQ-WL	1000 ~1500	100~150		100						
1002.75 ~1227.34	101.00	Diamond	HQ-WL	1000 ~1500	100	28.3/37.9 ~ 33.2/36.6	100	BH	5~30 ℓ/min at 1005.00m	None	–	Sandstone Shale	Core recovery: 99.4%

Table 3.2-2 Drilling Work of GTE-7

Items		Date: 1984 6	7	8	9	10	11	12	1985 1	2	3
Mobilization & Preparation		5 10									
Rig Up	Foundation Works	11 17									
	Rig Up	11	15								
Drilling	0m ~ 4.20m		16 20								
	4.20m ~ 30.00m		21 31								
	30.00m ~ 200.00m			1	1						
	200.00m ~ 504.00m				2	17					
	504.00m ~ 1,002.75m					18			14		
	1,002.75m ~ 1,227.34m								15	26	
Well Logging	1st logging			27							
	2nd logging					12					
	3rd logging								7 10		
	4th logging										1 3
Measurement of hole deviation										27 28	
Demobilization											4 8

Table 3.2-3 Major Drilling Equipment of GTE-7 (1)

Item	Model	Specifications	Quantity
Drilling machine	KOKEN Model "GSR-100CL"	Dual-system type drill with rotary table & spindle Dimension: 5.525 m (L) x 2.2 m (W) x 3.53 m (H) Weight: 10 t Drilling depth: 2,000 m (HQ rod) 1,500 m (3½" drill pipe) Hoisting capacity: 60 t Spindle rotation: 35 ~ 730 rpm Spindle torque: 1,250 kg.m (max) Table rotation: 15 ~ 290 rpm Total torque: 1,900 kg.m	1 set
Engine for drilling machine	NISSAN Model "PD-6-04"	Water-cooled diesel engine Dimension: 1.38m (L) x 0.805 m (W) x 1.23 m (H) Weight: 820 kg No. of cylinders: 6 cylinders Capacity: 142 HP/1,800 rpm Total stroke volume: 10,308 cc	1 set
Hydraulic power unit for drilling machine	KOKEN Model "GSR-100C-100CL"	Dimension: 3 m (L) x 1.1 m (W) x 1.6 m (H) Weight: 2,000 kg Oil pump: Tandem type geared pump: ℓ 30 ℓ/min (210 kg/cm^2) or 90 ℓ/min (50 kg/cm^2) Geared pump: ℓ 24 ℓ/min (100 kg/cm^2)	1 set
Engine for hydraulic power unit	NISSAN Model "FD-6-04"	Water-cooled diesel engine Dimension: 0.874m(L) x 0.725m(W) x 0.761m(H) Weight: 477 kg No. of cylinders: 6 cylinders Capacity: 115 HP/2,700 rpm Total stroke volume: 5,654 cc	1 set
Drilling pump	KOKEN Model "MG-75A"	Dimension: 4.2 m (L) x 1.1 m (W) x 2.27 m (H) (with engine) Weight: 3,800 kg Discharge capacity: 920 ℓ/min Working pressure: 40 kg/cm^2 Stroke length: 170 mm Cylinder bore: 155 mm	1 set
Power unit for drilling pump	NISSAN Model "PD-6-04"	The same as the engine for the drilling machine	1 set

Table 3.2.3 Major Drilling Equipment of GTE-7 (2)

Item	Model	Specifications	Quantity
Drilling pump (for coring)	KOKEN Model "MT-25"	Dimension: 2.72m(L) x0.74m(W) x 1.45m(H) Wight: 1,300 kg Discharge capacity: 35 ~ 280 ℓ/min Working pressure: 70 kg/cm^2 Stroke length: 130 mm Cylinder bore: 89 mm	1 set
Power unit for drilling pump (for coring)	MITSUBISHI Model "4DR 5"	Water-cooled diesel engine Dimension: 0.773m(L) x 0.64m(W) x 0.858m(H) Weight: 255 kg No. of cylinders: 4 cylinders Capacity: 35 HP/1,800 rpm Total stroke volume: 2,659 cc	1 set
Wireline hoist	Model "WLH-HD"	Dimension: 2,100mm(L) x 1,200mm(W) x 900 mm (H) Drum capacity: 8 mm x 1,600 m Hoisting capacity: 3.5 t Power unit: Motor, 15KW-4P, 60Hz, 220V	1 set
Mud mixer	Model "HT-750"	Dimension: 2.8 m (L) x 1.47 m (W) x 1.65 m (H) Weight: 780 kg Tank capacity: 710 ℓ x 2 Mixing capacity: 600 ℓ x 2 Propeller revolution: 500 ~ 600 rpm Power unit: Motor, 11Kw-4P, 60Hz, 220V	1 set
Mud screen	Model "IM-10B"	Dimension: 2.0 m (L) x 0.93 m (W) x 1.0 m (H) Weight: 400 kg Capacity: 1 m^3/min Power unit: Motor, 1.5Kw-4P, 60Hz, 220V	1 set
Water supply pump	Model "YSMK-5-80"	Turbine pump Discharge capacity: 0.35 ~ 0.71 m^3/min Head: 84 ~ 124 m Power unit: MITSUBISHI Model "4DR5" water-cooled diesel engine 35HP/1,800 rpm, 4 cylinder, 2,659 cc	1 set
Sand pump	Model "HS-48C"	Discharge capacity: 1,000 ℓ/min Head: 10 m Motor: 5.5Kw-4P, 60Hz-220V	1 set
	Model "HS-35"	Discharge capacity: 500 ℓ/min Head: 12 m Motor: 3.7Kw-4P, 60Hz-220V	1 set

Table 3.2-3 Major Drilling Equipment of GTE-7 (3)

Item	Model	Specifications	Quantity
Sand pump	Model "HS-615B"	Discharge capacity: 1,500 ℓ/min Head: 15 m Motor: 11Kw-4P, 60Hz-220V	1 set
Blowout preventer	Model "8-2000"	Dimension: 699 mmφ x 806 mm (H) Weight: 1,043 kg Seal-off range: 0 ~ 227 mm Working pressure: 140 kg/cm^2	1 set
Engine generator	Model "EDG60"	Dimension: 2.6 m(L) x 0.95 m (W) x 1.43 m (H) Weight: 1,870 kg Output: 60/73 KVA Frequency: 50/60Hz Voltage: 200/220V No. of phase: 3 phases Power unit: Model "DS-70" water-cooled diesel engine, 90HP/1,800 rpm	1 set
Winch	Model "RK-75TB"	Capacity: 4.5 t x 64 m/min Power unit: Model "6BD1" diesel engine 108 HP/2,200 rpm	1 set
	Model "SW-1015"	Capacity: 1.5 t Power unit: Model "TS-105C" diesel engine 9 HP/2,200 rpm	1 set
Agitator	TAKEUCHI Model "TVCP-0303-10"	Impeller diameter: 600 mm Impeller revolution: 88rpm Power unit: Motor, 2.2Kw-4P, 60Hz, 220V	1 set
Mortal mixer	Model "KNM-3"	Mixing capacity: 0.085 m^3 Drum revolution: 41 rpm Power unit: Robin Model "EY-1803B" gasoline engine, 35 HP/1,800 rpm	1 set
Cooling tower	Forced cooling type	Dimension: 1 m (L) x 1 m (W) x 5 m (H) Weight: 850 kg Capacity: 1 m^3/min	1 set
Derrick	Steel frame derrick	Dimension: 6.7 m (L) x 6.7 m (W) x 23.0 m (H) Critical load: 50 t	1 set
Substructure	Steel frame substructure	Dimension: 6.7 m (L) x 6.7 m (W) x 3.0 m (H) Critical load: 50 t	1 set
Crane carrier	Model "YFC22(Q)E"	Lifting capacity: 2,000 kg Lifting head: 4.9 m Loading capacity: 1,300 kg Engine output: 11 HP/2,000 rpm	1 set

Table 3.2.3 Major Drilling Equipment of GTE-7 (4)

Item	Type	Specifications	Quantity consumed
Hoisint	C-16B		1 set
Water	DHB-4		1 set
Swivel	RGB-30	Capacity: 30 t	1 set
Hoisting Swivel	B-N08	Capacity: 30 t	1 set
Hook block	TRB-35F-3	Capacity: 35 t Wheel: 3 Wheel size: 450 m/m	1 set
Rotary slip	For drill pipe	3-1/2", NQ	1 set
	For drill color	4-3/4", 6-1/4"	1 set
	For casing	6", 4-1/2"	1 set
Casing band		10"	2 sets
		8"	2 sets
		3-1/2"	1 set
Drill collor sefty clamp	11 rings		1 set
Bit breaker		12-1/4", 9-5/8", 7-5/8", 5-5/8"	each 1 set
Elevator	For drill pipe	3-1/2"	1 set
	For casing	4-1/4"	1 set
Elevator link		Capacity: 35 t	1 set
Rotary tong	"C" type	2-3/8" ~ 8-5/8"	1 set
Coring tools	HIG		1 set
Drilling pipe		3-1/2" IF x 120.7 m/m x 3 m	5 pcs
	HWY	Drilling rod (2-7/8" IF x 88.9 m/m x 6 m)	170 pcs
	3-1/2" DP	3-1/2" x 13.30 lb/ft Grade 6 m	50 pcs
	HQ-WL	HTG 6 m	280 pcs
	BQ-WL	6 m	100 pcs
Drill color		6-1/4" OD x 2-13/16" ID x 6 m 123.6 kg/m	6 pcs
		4-3/4" OD x 2-1/4" ID x 6 m 70 kg/m	8 pcs
Stabilizer	Wing. welding type 4 wings	9-5/8"	3 pcs
		7-5/8"	3 pcs
		5-5/8"	2 pcs
Lift sub		3-1/2" x 2-3/8" IF (P)	2 pcs
		3-1/2" x 3-1/2" IF (P)	3 pcs
		3-1/2" x 4" IF (P)	3 pcs
Cementing head	For single stage cementing by two-plug method	8"	1 set
		6"	1 set
		4-1/2"	1 set
Mud testing tools		Sand content, mud balance, shearometer funnel viscometer, filter press, etc.	1 set
Disc grinder			2 sets
Electric drill			1 set
Chain saw			1 set
Other tools			1 set

Table 3.2.4 Consumables of Materials of GTE-7 (1)

Bit and Casing pipe

Item	Type	Specifications	Quantity consumed
Bit	SEKISUKU tricone bit	12-1/4", MH	1 pc
		9-5/8", MH	2 pcs
		9-5/8", V3F	1 pc
		7-5/8", MH	3 pcs
		7-5/8", V3F	2 pcs
		5-5/8", MH	5 pcs
		5-5/8", V3F	4 pcs
		3-7/8", M	2 pcs
	HQ-WL		
	diamond bit	45 ct	60 pcs
	diamond reamer		9 pcs
Casing pipe	Flush joint, blind pipe	14" SGP	4.20 m
		10" SGP	28.10 m
		8" STPG-38, sch-40	199.00 m
		6" STPG-38, sch-40	501.00 m
		4-1/2" STO-J-55 x 10.50 lb/ft	998.00 m

Table 3.2.4 Consumables of Materials of GTE-7 (2)

Mud materials, Cement and Oil & Fats

Item	Type	Quantity consumed	Remarks
Mud material	Bentonite	37,375.00 kg	25 kg/sack x 1,495.00 Sacks
	Libonite	6,900.00 kg	20 kg/sack x 345.00 Sacks
	Telnite BH	10,110.00 kg	20 kg/sack x 505.50 Sacks
	CMC TE-DS	70.75 kg	20 kg/sack x 3.54 Sacks
	Super ashestos	2,182.00 kg	15.87 kg/sack x 137.50 Sacks
	Tel flow	740.00 kg	20 kg/can x 37.00 Cans
	Soda ash	916.50 kg	40 kg/sack x 22.91 Sacks
	Mud oil	320.00 kg	16 kg/can x 20.00 Cans
	Tel seal	100.00 kg	10 kg/sack x 10.00 Sacks
	Tel stop P	75.00 kg	25 kg/sack x 3.00 Sacks
Cement	Portland cement	18,000.00 kg	40 kg/sack x 450.00 Sacks
	Coothermal well cement	29,560.00 kg	40 kg/sack x 739.00 Sacks
	Dispersant CFR-2	97.70 kg	
	Retarder HR-4	17.50 kg	
Oil & fats	Diesel oil	108,200.00 ℓ	
	Gasoline	220.00 ℓ	
	Grease	345.00 kg	
	Hydraulic oil	400.00 ℓ	
	Lubricating pil	840.00 ℓ	
	Gear pil	210.00 ℓ	

Table 3.2-5 Breakdown of Drilling Work of GTE-7

Depth	Work Items	Period	No. of calendar days	No. of working days	Other days
0.00 m ~ 4.20 m	14" SCT (0.00 m ~ 4.20 m)	1984 Jul. 16 ~ Jul. 20	5	4	1
4.20 m ~ 30.00 m	12-1/4" T.B (4.20 m ~ 13.14 m)	Jul. 21	1	1	0
	Pre. of HQ-WL coring	Jul. 22	1	1	0
	HQ-WL coring (13.14 m ~ 16.78 m)	Jul. 23	1	1	0
	12-1/4" T.B (13.14 m – 30.00 m)	Jul 24 ~ Jul. 26	3	3	0
	10" CP insertion, cementing waiting and waiting and reaming	Jul. 27 ~ Jul. 31	5	5	0
	Total		16	15	1
30.00 m ~ 200.00 m	HQ-WL coring (30.00 m ~ 57.12 m)	Aug. 1 ~ Aug. 2	2	2	0
	7-5/8" T.B reaming (30.00 m ~ 57.12 m)	Aug. 3	1	1	0
	Cementing	Aug. 4	1	1	0
	7-5/8" T.B reaming	Aug. 5	1	1	0
	HQ-WL coring (57.12 m ~ 64.89 m)	Aug. 6	1	1	0
	7-5/8" T.B reaming, cementing	Aug. 7 ~ Aug. 8	2	2	0
	HQ-WL coring (64.89 m ~ 201.00 m)	Aug. 9 ~ Aug. 18	10	10	0
	Inspection of the machines	Aug. 19	1	1	0
	9-5/8" T.B (30.00 m ~ 200.00 m)	Aug. 20 ~ Aug. 26	7	7	0
	1st logging	Aug. 27	1	1	0
	8" CP insertion, cementing, waiting and reaming	Aug. 28 ~ Sep. 1	5	5	0
	Total		32	32	0
200.00 m ~ 504.00 m	HW-WL coring (200.00 m ~ 504.69 m)	Sep. 2 ~ Sep. 24	23	23	0
	Inspection of the machines	Sep. 25	1	1	0
	7-5/8" T.B (200.00 m ~ 504.00 m)	Sep. 26 ~ Oct. 11	16	16	0
	2nd logging	Oct. 12	1	1	0
	6" CP insertion, cementing, waiting and reaming	Oct 13 ~ Oct. 17	5	5	0
	Total		46	46	0
504.00 m ~ 1002.75 m	HQ-WL coring (504.69 m ~ 1002.75 m)	Oct. 18 ~ Dec. 10	54	54	0
	Prep. of 5-5/8" reaming	Dec. 11 ~ Dec. 12	2	2	0
	5-5/8" (504.00 m ~ 1002.75 m)	Dec. 13 ~ 1985 Jan. 2	21	21	0
	Waiting for logging	Jan. 3 ~ Jan. 5	3	3	0
	Reaming	Jan. 6	1	1	0
	3rd logging	Jan. 7 ~ Jan. 10	4	4	0
	4-1/2" CP insertion, waiting and reaming	Jan. 11 ~ Jan. 14	4	4	0
	Total		89	89	0
1002.75 m ~ 1227.34 m	HQ-WL coring (1002.75 m ~ 1225.99 m)	Jan. 15 ~ Feb. 22	39	39	0
	Machine maintenance	Feb. 23 ~ Feb. 24	2	2	0
	HQ-WL coring (1225.99 m ~ 1227.34 m)	Feb. 25 ~ Feb. 26	2	2	0
	Total		43	43	0
	Grand Total		226	225	1

Table 3.2-6 Details of Cementing of GTE-7

(1) Casing Piep Cementing

Casing step	1st step	2nd step	3rd step	4th step	5th step	Remarks
Nominal dia. x depth	14B × 4.20 m	10B × 28.10 m	8B × 199.00 m	6B × 501.00 m	4½B × 1,000.00 m	Geothermal cement was used from the 3rd step 3rd step setting retarder: 0.35% dispersent: 0.35% 4th and 5th step setting dispersant: 0.35%
Volume of clearance between well and casing	5 L	776 L	2,355 L	4,591 L	6,821 L	
Q'th of slurry pressed in	444 L	1,570 L	4,180 L	7,124 L	12,040 L	
Q'ty of cement used	520 kg	1,840 kg	5,000 kg	8,520 kg	14,400 kg	
Specific gravity	1.80	1.80	1.80	1.80	1.80	
Setting time	17 h	65 h	64 h	78 h	50 h	
Method	Pouring in from well head	one-plug method	two-plug method	two-plug method	one-plug method	

(2) Plug Buck Cementing

Depth of well bottom	Purpose	Q'ty injected	Method	Cement head	Result
19.00 m	Preventing cave-in	1,080 kg	Flushed through HQ rod	10.95 m	Success
57.12 m	Preventing cave-in	1,440 kg	Flushed through HQ rod	23.50 m	Success
64.89 m	Preventing cave-in	1,320 kg	Flushed through HQ rod	32.25 m	Success
200.00 m	Reinforcing	880 kg	Squeezed through HQ rod with 30 kg/cm^2	184.52 m	Success

Table 3.2-7 Atmospheric Temperature and Circulation Temperature of GTE-7 (1)

Depth	Atmospheric Temp. (°C)		Circulation Temp. (°C)	
	Highest	Lowest	Income	Outgoing
50.00	35.0	27.0	40.9	39.5
89.89	35.0	25.0	43.4	44.9
118.94	35.0	27.0	46.6	46.4
150.74	32.0	26.0	45.4	42.8
180.24	34.0	25.0	47.5	48.2
210.59	32.0	24.0	47.7	48.0
250.74	36.0	26.0	45.5	51.0
277.54	33.0	24.0	38.8	44.0
299.39	32.0	24.0	37.7	42.0
330.24	34.0	23.0	37.0	45.0
358.84	34.0	24.0	38.0	43.0
389.14	34.0	24.0	37.0	44.0
419.99	34.0	24.0	38.0	44.5
450.04	32.0	24.0	37.2	45.5
480.14	34.0	25.0	37.8	42.2
510.69	30.0	25.0	34.3	44.2
540.54	28.0	23.0	33.3	45.1
570.69	31.0	23.0	33.9	43.6
600.49	32.0	16.0	32.8	43.7
629.74	30.0	17.0	31.1	44.5
661.49	31.0	19.0	36.0	43.3
689.24	32.0	20.0	37.8	42.8
720.44	32.0	20.0	33.7	43.7
749.39	32.0	20.0	35.7	42.4
780.19	32.0	19.0	37.1	43.7
810.64	33.0	18.0	33.4	42.0
840.19	31.0	20.0	34.5	44.7
869.99	30.0	14.0	34.0	38.8

Table 3.2-7 **Atmospheric Temperature and Circulation Temperature of GTE-7 (2)**

Depth	Atmospheric Temp. (°C)		Circulation Temp. (°C)	
	Highest	Lowest	Income	Outgoing
900.09	30.0	18.0	34.6	46.9
929.64	30.0	14.0	34.8	44.0
961.14	28.0	14.0	35.6	43.8
990.19	29.0	10.0	36.3	43.9
1019.99	30.0	8.0	28.3	37.9
1049.34	32.0	11.0	37.3	42.4
1080.49	30.0	16.0	34.5	39.2
1109.89	32.0	20.0	34.5	38.5
1140.19	33.0	13.0	33.9	38.0
1170.94	33.0	12.0	34.7	37.3
1200.09	35.0	14.0	33.5	38.3
1227.34	35.0	15.0	33.2	36.6

Table 3.2-8 Bottom Hole Temperature of GTE-7 (1)

Date of Measurement	Depth (m)	Temperature (°C)			
		Thermometer (I)	Thermometer (II)	Thermometer (III)	Average
Aug. 2, '84	50.00	43.0	43.0	43.0	43.0
11	89.89	46.0	46.0	46.0	46.0
13	118.94	48.0	49.0	49.5	48.8
15	150.74	48.0	49.5	50.0	49.2
17	180.24	51.5	50.0	51.5	51.0
Sep. 3	210.59	50.0	51.0	52.0	51.0
6	250.74	53.0	52.0	52.0	52.3
8	277.54	46.0	47.0	48.0	47.0
10	299.39	48.0	48.0	49.0	48.3
12	330.24	50.0	50.0	50.0	50.0
14	358.84	54.0	52.0	52.0	52.7
16	389.14	54.0	55.0	57.0	55.3
18	419.99	55.0	58.0	60.0	57.7
20	450.04	60.0	62.0	61.0	61.0
22	480.14	65.0	64.0	67.0	65.3
Oct. 18	510.69	60.0	63.0	63.0	62.0
21	540.54	57.0	59.0	59.0	58.3
22	570.69	62.0	59.0	63.0	61.3
25	600.49	64.0	65.0	67.0	65.3
28	629.74	69.0	69.0	70.0	69.3
30	661.49	68.0	70.0	70.0	69.3
Nov. 2	689.24	68.0	73.0	71.0	70.7
5	720.44	74.0	72.0	73.0	73.0
7	749.39	78.0	78.0	83.0	79.7
13	780.19	78.0	81.0	83.0	80.7
18	810.64	80.0	83.0	82.0	81.7
22	840.19	79.0	83.0	85.0	82.3
25	869.99	83.0	84.0	88.0	85.0
29	900.09	82.0	83.0	86.0	83.7

Table 3.2-8 Bottom Hole Temperature of GTE-7 (2)

Date of Measurement	Depth (m)	Temperature (°C)			
		Thermometer (I)	Thermometer (II)	Thermometer (III)	Average
Dec. 2	929.64	82.0	84.0	88.0	84.7
6	961.14	85.0	85.0	86.0	85.3
9	990.19	86.5	87.0	88.5	87.3
Jan. 17, '85	1019.99	90.0	90.0	81.0	87.0
22	1049.34	94.0	94.0	94.0	94.0
28	1080.49	95.0	95.0	99.0	96.3
30	1109.89	96.0	95.0	99.0	96.7
Feb. 3	1140.19	100.0	98.0	97.0	98.3
8	1170.94	98.0	97.0	97.0	97.3
13	1200.09	99.5	102.0	98.0	99.8
26	1227.34	101.0	103.0	98.5	100.8

Table 3.2-9 Records of Tricone Bits of GTE-7 (1)

No.	Diameter (mm)	Drilling Depth (m)	Drilling length (m)	Net drilling time (h)	Penetration rate (m/h)	Remarks
MH-1279-S	311.2	0.00 ~ 2.60	2.60	1.50	1.73	drilling the mouse hole
		4.20 ~ 13.14	8.94	4.50	1.99	
		13.14 ~ 30.00	16.86	11.75	1.43	13.14 ~ 16.78 reaming
		Total	28.40	17.75		
MH-1105-S	244.5	27.45 ~ 30.00	2.55			drilling out cement
		30.00 ~ 64.89	34.89			
		64.89 ~ 96.83	31.94			
		Total	69.38	28.75		
V3F 1587S	244.5	96.93 ~ 163.75	66.92	61.83	1.08	
MH-1104-S	244.5	163.75 ~ 200.00	36.25	41.30	0.88	
MH-7008-S	193.7	0.00 ~ 5.00	5.00	2.00	2.50	drilling the rat hole
		24.12 ~ 30.00	5.88	3.00	1.96	drilling out the cement
		30.00 ~ 57.12	27.12	20.00	1.36	reaming
		23.00 ~ 57.12	34.12	8.00	4.27	drilling out the cement
		57.12 ~ 64.89	7.77	8.00	0.97	reaming
		32.25 ~ 64.89	32.64	9.00	3.63	drilling out the cement
		184.52 ~ 200.00	15.48	4.00	3.87	drilling out the cement
		200.00 ~ 224.15	24.15	20.83	1.16	reaming
		Total	152.16	74.83		
M 7309	98.4	200.00 ~ 200.75	0.75	4.00	0.19	drilling the center of the hole
MH-7009-S	193.7	224.15 ~ 301.21	77.06	59.67	1.29	
V3F 6013F	193.7	301.21 ~ 391.04	89.83	77.92	1.15	
V3F 6012S	193.7	391.04 ~ 485.23	94.19	136.83	0.69	
MH-7010-S	193.7	485.23 ~ 504.00	18.77	19.00	0.99	

Table 3.2-9 Records of Tricone Bits of GTE-7 (2)

No.	Diameter (mm)	Drilling Depth (m)	Drilling length (m)	Net drilling time (h)	Prenetration rate (m/h)	Remarks
MH-8656-S	142.9	480.90 ~ 504.69	23.79	13.75	1.73	drilling out the cement
		504.69 ~ 535.83	31.14	16.00	1.95	
		Total	54.93	29.75		
MH-8658-S	142.9	535.83 ~ 584.20	48.37	67.00	0.72	
MH-8659-S	142.9	584.20 ~ 648.08	63.88	63.33	1.01	
MH-8657-S	142.9	648.08 ~ 710.23	62.15	32.92	1.89	
V3F 7743S	142.9	710.23 ~ 800.23	90.00	56.92	1.58	
V3F 7745S	142.9	800.23 ~ 879.83	79.60	45.75	1.74	
V3F 7742S	142.9	879.83 ~ 940.73	60.90	45.17	1.35	
V3F 7741S	142.9	940.73 ~ 1002.75	62.02	44.08	1.41	
MH-8660-S	142.9	770.00 ~ 1002.75	232.75	15.00		reaming
M 7308	98.4	936.69 ~ 1001.80	65.11	19.50	3.33	drilling out the cement

Table 3.4-2 Result of Microscopic Observation of GTE-7

Depth (m)	Rock Name	Allogenic and Authigenic Minerals										Alteration and Vein Minerals						Remarks
		Qz	Kf	Pl	Sp	Zr	Tm	Ap	Se	Ch	Cb	Cb	Qz	Se	Ch	Kf	Oq	
70.5	Grey med. grained s. st.	◎	△	◎	●	●	●		△	△		○		●	●		●	Moderate carbonatination (disseminated)
146.80	Grey fine grained st.	◎		○	●	●	●		○	○		●					△	Faint carbonate stringer
217.00	Black greay mud st.	◎		●	●				◎	◎		●	●				△	Faint quartz vein with carbonate mineral
348.00	Black greay mud st.	◎		●	●				◎	◎		●					△	Faint carbonate stringer
402.00	Black mud st.	◎		●	●			●	○	○		●					◎	Faint stringer/dissemination of carbonate. Slightly wide stringer/dissemination of pyrite
531.00	Black greay mud st.	◎							◎	○		●	△				◎	Carbonate minerals in quartz vein
610.50	Grey med. grained s. st.	◎		△					○	○		○		●	●		△	Moderate carbonatization (dissemination/vein)
663.00	Black calcureous mud st.	○							△	△	△	◎					◎	Moderate carbonatization (dissemination/vein). Slightly wide stringer
721.00	Grey limestone	○		●					●		◎	●					○	Faint carbonate stringer
832.00	Black mud st.	◎							◎	◎		△					○	Faint to moderate carbonate stringer. Slightly wide strnger/dissemination of pyrite
905.00	Grey calcareous s. st.	◎	●	○					●	●	◎						●	
1,031.70	Grey fine grained s. st.	◎	●		●		●		◎	●		○	●				●	Moderate carbonatization (dissemination/vein)
1,094.00	Grey white med. grained s. st.	◎	○	●	●	●		●	●								●	Dissemination of macroscopic pyrite
1,213.50	Grey med. grained s. st.	◎	○	●	●	●			○			○			△	△	●	Moderate carbonatization (dissemination/vein)

Abbreviations: Qz : Quartz, Kf : K-feldspar, Pl : Plagioclase, Sp : Sphene, Zr : Zircon, Tm : Tourmaline, Ap : Apatite, Se : Sericite, Ch:: Chlorite, Cb : Carbonate, Oq : Opaque

Symbols: ◎ : Abundant, ○ : Common, △ : Rare, ● : Very rare

Table 3.4-3 X-ray Diffraction Data of GET-7

Samples	Well	Depth (Mineral →)	Quartz	Calcite	Dolomite	Aukerite	Plagioclase	K-feldspar	Smectite	Sericite	Chlorite	Kaolinite	Palygorskite	Pyrite	Marcasite	Hematite	Goethite	Gypsum	Fluorite
No. 7	GTE-7	70.05 m	◎	Δ			◎			● 2M	Δ								
No. 13	GTE-7	146.80 m	◎	Δ			◎			Δ 2M	○			●					
No. 21	GTE-7	217.00 m	◎	◎	○					●	●			●					
No. 28	GTE-8	330.00 m	◎	○						○	Δ			Δ				Δ	
No. 33	GTE-7	402.00 m	◎				Δ			Δ 2M	Δ			Δ					
No. 33	GTE-7	531.00 m	◎							Δ 1M2M	○			Δ					
No. 44	GTE-7	610.50 m	◎	Δ			○			Δ 2M	○								
No. 46	GTE-7	663.00 m	◎	Δ			Δ			Δ 2M	Δ			Δ					
No. 49	GTE-7	721.00 m	◎	◎				Δ		Δ	Δ			●					
No. 54	GTE-7	832.00 m	◎							○ 2M	Δ			Δ					
No. 57	GTE-7	905.00 m	◎	◎						Δ	Δ								Δ
No. 62	GTE-7	1,031.70 m	◎					Δ		Δ 1M2M		Δ		●					
No. 65	GTE-7	1,094.00 m	◎	●				○		Δ		Δ		Δ					
No. 71	GTE-7	1,213.50 m	◎	●				○		●	○								

◎ : Much ○ : Common Δ : Few ● : Very Rare

Table 3.4-4 Result of Geophysical Measurement of GTE-7

No.	Depth	Rock Name	Density	Density	Density	Porosity	Magnetic Susceptibility	Thermal Conductivity
			Natural condition	Dry condition	Wet condition			
	(m)		g/cm^3	g/cm^3	g/cm^3	%	EMU/CC	$\times 10^{-3}$ cal/cm·sec·°C
1	70.04	Grey sandstone	2.67	2.67	2.68	1.39	1.19×10^{-5}	9.046
2	146.8	Black shale	2.71	2.71	2.72	0.99	1.61×10^{-5}	8.701
3	217.0	Black shale	2.69	2.68	2.69	0.68	1.50×10^{-5}	10.735
4	348.0	Black shale	2.68	2.67	2.69	2.89	9.25×10^{-6}	6.571
5	402.0	Black shale	2.63	2.62	2.66	4.11	6.34×10^{-6}	8.021
6	543.5	Grey chert	2.71	2.71	2.71	0.55	6.84×10^{-6}	11.020
7	610.5	Grey sandstone	2.73	2.72	2.73	1.22	1.93×10^{-5}	7.832
8	663.0	Black shale	2.74	2.72	2.75	3.27	1.00×10^{-5}	6.951
9	721.0	Grey limestone	2.70	2.69	2.70	1.48	8.19×10^{-6}	8.523
10	808.0	Grey chert	2.65	2.65	2.65	0.33	3.38×10^{-5}	17.306
11	905.0	Limestone	2.65	2.65	2.66	1.06	1.13×10^{-5}	9.171
12	1064.7	Black shale	2.64	2.64	2.64	0.36	1.46×10^{-5}	13.521
13	1094.0	Siliceous sandstone	2.41	2.39	2.47	8.32	8.66×10^{-6}	10.684
14	1213.5	Siliceous sandstone	2.65	2.64	2.65	0.98	1.46×10^{-5}	13.013
		Mean Value $\bar{X}$	2.66	2.65	2.67	1.97	1.32×10^{-5}	10.078
		Number of Sample n	14	14	14	14	14	14
		Standard Deviation σ	0.08	0.08	0.07	2.15	0.70×10^{-5}	2.93

4. Supplementary Survey for detecting Geothermal Reservoir

4.1 Generalization

The exploratory well GTE-7 was drilled by the JICA study team to a depth of 1227.3 m in 1984, as the third phase of survey for the San Kampaeng geothermal development study. The GTE-7 well, however, failed to provide ample data to evaluate the geothermal reservoir of this area. The core logging data were reexamined and as a result of that study, recommended supplementary survey including both fault detection and underground temperature survey were conducted centering on the hot water discharging zone and including the area of geothermal manifestation 1985.

Objective of the study is to delineate the geothermal reservoir and to judge the necessity for a further drill hole, GTE-8, planned by EGAT, and to recommend a suitable bore hole location in the event that the additional drill hole is thought to be worthwhile. The fingerprint method, a geochemical prospecting method using soil gas, was adopted for the fault detecting survey by members of the JICA study team. EGAT conducted subsurface temperature survey using ten drill holes of 100 meters depth and complied an isotherm contour map at the depth of 100 meters. The results of survey and interpretation thereof will be described in the following sections.

4.2 Fault Tracing Survey by Fingerprint

4.2.1 Method of Survey

(1) Outline

The fingerprint method is a geothermal prospecting method using soil gas, and is composed of the following three techniques: soil gas collection, pyrolysis mass spectrometer analysis and multivariate statistical analysis.

The merits of the method are the following two points:

① The effect of short time fluctuation of gas density is omitted through the integration of gas collection over a certain period.

② Instead of analysing one or a few specified gas components, multi components are analysed, relative abundances of each component are identified and the spectrum patterns are compared (Fig. 4.2-1).

Flow of survey works is as follows:

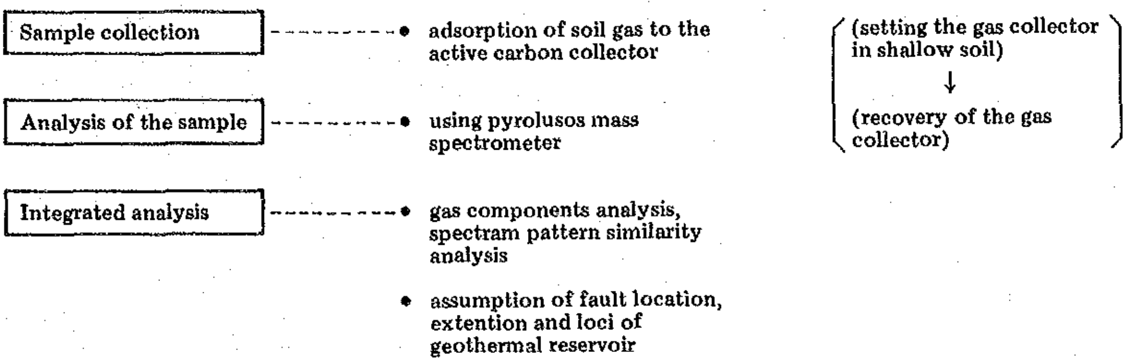

Fig. 4.2-1 Flow Chart of Fingerprint Geothermal Survey

(2) Sampling method

A gas collector, which is composed of a glass tube containing iron wire bar coated with active carbon powder, is buried with open side down within 30 cm depth of the hole dug by hand-auger.

The collector is left for more than one week to adsorb upward migrating gas. This serves to eliminate the effect of short time gas fluctuation and at the same time to condensate very minute amounts of gas components. After leaving the collector for a suitable period, it is recovered, immediately fitted with air-tight capping and sent to the laboratory.

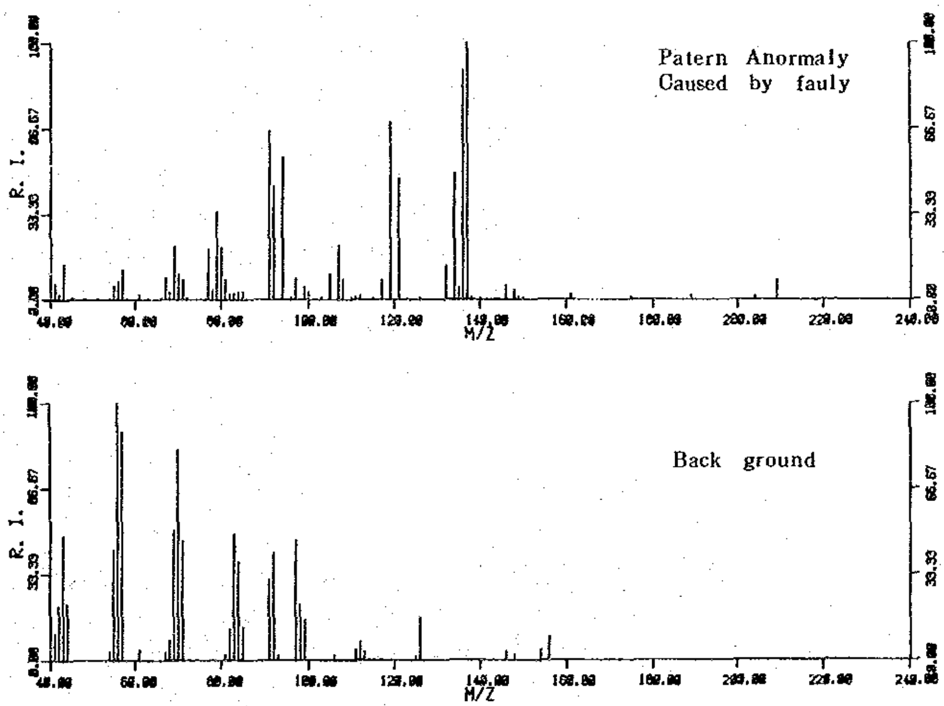

Fig. 4.2-2 Mass Spectrum in Fingerprint Analysis

(3) Analytical method

The gas analysis is conducted for mass umber/electricity 29 to 240 using a pyrolysis-mass spectrometer connected with a computer system. A mass spectrum thus obtained is shown in Fig. 4.2-2. Y axis demonstrates relative intensity (R.I.) of the spectrum and X axis stands for a ratio of ion mass number (a.m.u.)/unit electric charge number (mass/electric charge) with increasing mass of ions towards the right. R.I. means that each spectrum is normalized against the maximum spectrum height as 100%.

(4) Data Analysis

A mass spectral pattern, called a fingerprint, obtained from a fault has the following two characteristics: it has many peaks in the higher mass zone and a higher amount of gas flux, shown as total ion content when analysed. The high molecular weight gas considered to be generated deep in the ground passes more easily through open cracks than densely packed geological strata. Thus the fingerprint with high molecular weight will designate the loci of faulting.

1) High molecular weight gas flux ratio

In addition to a visual evaluation of the fingerprint, High Molecular Weight Gas Flux ratio is also examined. HMWGFR is defined as the following equation.

HMWGFR = summation of ion count $M/\Sigma \geqq 120$/modified total ion count $\times 100$

2) Modified Total Ion Count

Modified Total Ion Count is defined by subtracting the ion count of atmospheric components from the total ion count of the mass spectrum.

MTIC stands for the total gas flux emanating from the underground where the gas collector is placed. Total gas flux, which is proportional to total ion count, will increase when the gas emanates from deep underground through fault and fracture channels.

3) Similarity analysis using multivariate statistical analysis

Each peak of the mass spectrum, or fingerprint, reflects a specified gas component. Similarity analysis is a method to approximate the ratio of amounts of each gas component. Existence and extent of a geothermal area can be presumed by the similarity analysis adopting a model zone which presents a known geothermal field. In this survey, a model area is selected where the most active geothermal manifestation is observed and similarity study based on this model area was conducted.

4.2.2 Result of Survey

(1) Field survey

A total of 359 gas collectors were placed, each at 20 meter intervals, on the rectangular E-W and N-S survey lines with a line spacing of 200 and 400 meters. Of these, 24 collectors were lost and/or contaminated by insects and the balance of 335 samples were analysed.

(2) Results

Identification of fault and fracture:

① Abnormal gas components

Fault and fissure indicating samples, which contain abundant mass spectral peaks in the higher molecular weight region and higher total ion count, amount to 41 samples.

After studying the distribution of the above-mentioned 41 samples in the survey area, the fault pattern and continuity of each fault were estimated.

Fig. 4.2-3 shows the estimated 9 faults; NW-SE : 4
NE-SW : 3
N-S : 2

② High molecular weight gas flux ratio (HMWG flux ratio)

The HMWG flux ratios in this area are a minimum of 0%, a maximum of 44% and average 2.3%. Fig. 4.2-4 shows the area where this ratio is more than 2.5% as a high molecular weight gas concentrated zone. The anomalous zone stretches in NW-SE direction from the center of the survey area to the southeastern part of the area.

③ Total ion count (TIC)

TIC indicates a minimum ion count of 4,656, a maximum of 1,083,756 and an average of 81,259. Fig. 4.2-5 shows a highly anomalous TIC zone with a threshold value of 100,000. The anomalous zone shows distribution similar to that of HMWC flux ratio and occupies the central to south-eastern part of the survey area with NW-SE trending.

④ Similarity analysis using multivariate statistical analysis.

Model samples are seleoted from the area where temperature is more than 70°C at 20 m depth. Similarity analysis was performed for each sample, except for 41 fault and fissure designation samples, from the model samples using multivariate statistical analysis. Fig. 4.2-6 shows the area where the similarity value is more than 5. Higher similarity areas are distributed in two separate areas, one in the northwest and the other in the southeast of the survey area.

⑤ Low gas flux anomalous zone

A low gas flux anomalous zone, where ion count is less than 50,000 and high molecular weight gas flux ratio is less than 1, develops alteration on the surface or lacks faults or fractures. In such a zone gas migration is thought to be sealed.

A low gas flux anomalous zone occupies the northeastern part of the survey area, where numerous hot springs were observed and alteration at the surface is marked. Judging from this, the low gas flux anomalous zone reflects an alteration zone produced by outflowing hot springs.

4.2.3 Distribution of Fractures detected by Survey

(1) Fault and fissure

Geologic structure of the survey area is characterized by a north-south trending monoclinic structure (Fig. 4.2-7). Geochemical prospection using fingerprint method revealed the existence of three fault systems namely NW-SW and N-S system. Those faults divide the geological structure into blocks and also encircle the geothermal showings of the area. This implies that the fault systems have strong genetic relation with development of the geothermal reservoir.

(2) Geothermal reservoir

The combined anomalous zone of gas flux, both total gas flux anomaly or high molecular weight gas flux ratio anomaly and low gas flux anomaly which designate altered areas, are distributed in the southeast area and continue toward the northwest of the survey area. The combined anomalous zone takes a form of a NW-SE extending ellipse and is highly concordant to the zone of the high underground temperature revealed by the drillings of 100 meters depth. (Fig. 4.2-8)

The similarity zone is divided into two parts, one at the northwest and the other at the south. It is considered that the one in the northwest reflects alteration zone of shallow depth while the one in the south corresponds to the deep seated geothermal reservoir.

(3) Summary

Geochemical prospecting adopting the fingerprint method was carried out to detect faults and fissures and to study to possibility of existence of a geothermal reservoir in the survey area.

① A total of 359 collectors were placed in the ground and 335 were analysed.

② Forty one samples showed anomalous pattern suggesting fault and fissure. They were classified as three fissure systems: NW-SE, NE-SW and N-S system, with a total of nine fissures.

③ A total gas flux anomaly and high molecular weight gas flux ratio anomaly, both indicative of a deep seated geothermal reservoir, and low gas flux anomals which designates alteration of the subsurface, were detected from the northwest to the southeast of the survey area. These gas flux anomalies show NW-SE distribution in an ellipse form and imply a possibility of a sealed geothermal field in this area.

④ As a result of similarity analysis, a geothermal manifestation expressed by surface alteration was found in the northwest and a geothermal manifestation considered to originate from a deep seated heat reservoir was found at the south of the survey area.

4.3 Underground Temperature Survey

4.3.1 Heat Hole Drilling

The survey was carried out with cooperation of EGAT.

In parallel with fault tracing survey by the fingerprint method, drilling of ten heat holes was commenced from July 1985 for the purpose of measuring 100 m depth underground temperature.

Objective of this survey is to make an isothermal map for 100m depth from the surface and to know the relation between fault distribution and underground temperature distribution. For this purpose, heat holes were sited in the same area where fault tracing survey was performed. Location map of heat holes is shown in Fig. 4.3-1. Of the 10 heat holes, the one located 850 m south of the survey are is not included in Fig. 4.3-1. Due to the reason that, in the case of vapor or thermal water discharge from the hole, hole temperature does not correspond to the temperature of surrounding rock but rather that of the pouring fluid, fractures where circulation loss occurred were filled by cement. In addition, casing pipe was inserted to the bottom of hole to avoid temperature disturbance in the hole. Examples of completion of drilled holes are shown in

Fig. 4.3-2.

4.3.2 Measurement of Heat Holes

After drilling of each bore hole, hole temperature was measured several times. Fig. 4.3-3(1)-(3) shows vertical temperature distribution in each hole determined on the basis of data obtained over a long standing time such that hole temperature achieved an equilibrium state in relation to the surrounding geological formation.

Table 4.3-1 shows bottom hole temperature of each bore hole. Aside from heat holes, exploration wells GTE-2, GTE-5, GTE-6 and GTE-7 are located in the survey area. Among them, GTE-2 and GTE-5 discharged hot water and hole temperature thereat accordingly does not coincide with formation temperature. On the other hand, temperature conditions at the other exploration wells have achieved a static state with passage of time and are regarded as reflecting formation temperature.

Table 4.3-1 includes the data of exploration wells in a static state, and the isotherm for 100 m depth was drawn using all available data.

4.3.3 Distribution of Underground Temperature and Fault

Based on the measured values shown in Table 4.3-1, the isotherm at 100m depth is presented in Fig. 4.3-4. Fig. 4.3-5 shows the isotherm map superimposed upon fault distribution detected by the fingerprint method. The following can be deduced from the superimposed map.

① The high temperature zone with temperature above 70°C nearly coincides with the area occupied by two NW-SE trending faults, and direction of the high temperature zone conforms with that of the faults.

② The northern extension of high temperature zone is cut by a NW-SE trending fault. This means the fault plays a role as the boundary between high temperature (discharging) zone and low temperature recharging zone. This was as presumed on the basis of analysis of GTE-7 drilling results.

③ High temperature zones, of temperature more than 90°C, are found in two places: one in the geothermal manifestation area and the other at the southeast of the former. This coincides with the results of fingerprint survey. In particular, from the fact that No.9 heat hole shows high temperature of 112°C, it is possible to say that hot geothermal fluid may be stored in the area with a distribution of 500 m × 1,000 m+ which lies between to NW-SE trending faults.

④ In conclusion, it is summarized that presence of the geothermal reservoir in the San Kampaeng area was clarified by geochemical fault tracing and underground temperature survey.

Table 4.3-1 Bottom Temperature of Heat Holes and Bore Hole Temperature of Test Wells

Hole Number	Bottom Temperature	Depth
No. 5	40.3°C	100 m
6	98.2	100
7	79.6	102
8	43.6	92
9	112.3	99.5
10	62.2	102
11	78.0	92
12	40.7	100
13	37.0	100
14	48.1	94.5
Exploration Well No.	Hole Temperature at 100 m Depth	
GTE -2	–	
-5	44.2°C	
-6	–	
-7	60.0	

4.4 Summary

In the geothermal area composed of hard rocks, as in the case of San Kampaeng, geothermal fluid in the underground moves through cracks along faults or fractures. The target area of geothermal development therefore is focussed on the area with dominant fractures.

Geothermal survey such as the fingerprint method serves to detect the existence of faults or fractures covered by soil regardless of the underground temperatue. In the geothermal area, since geothermal fluid is stored in faults and fractures in the ground, a high temperature zone indicates such an area.

From the results of fault or fracture tracing survey and subsequent underground temperature survey at 100 m depth, it has become clear that a high temperature zone with temperature above 70°C coincides with the area of faults with NW-SE direction, which means that geothermal fluid is stored in the faults and fractures with same direction. In other words, the area and extent of the geothermal reservoir was roughly revealed.

This survey discloses the underground temperature up to 100 m depth, and deeper down a higher and wider area of geothermal reservoir could be expected. The geothermal reservoir area with temperature more than 70°C at 100 m depth is 500 m in width and more than 1,000 m in length.

The temperature of geothermal fluid stored in the above mentioned geothermal reservoir at a depth of 1,000 m or more is a critical factor in whether or not geothermal development in San Kampaeng is feasible.

If geothermal fluid has a temperature higher than 180°C, it is possible to generate power using geothermal steam, but if the temperature is lower than 180°C, for example 160°~180°C, other power generation such as the Binary Cycle System must be considered.

Consequently, whether geothermal development in the San Kampaeng is feasible or not hingers on the fluidal temperature in the reservoir.

Judging from the fact that the geochemical thermometer indicated fluidal temperature of 160°~200°C, and that a hlgh temperature of 120°C at the depth of 20 m was recorded in the geothermal manifestation area as well as the fact that the underground temperature survey this year disclosed a maximum temperature of 112°C in the southeastern portion of the manifestation area, it can be said that drilling another exploration well is warranted to obtain data on fluidal temperature and rock permeability. In conclusion, the survey results of 1985 are summarized as follows:

(1) From the analytical results of logging data, it was deduced that the GTE-7 drilling site is located at a recharge area of thermal water.

(2) Also it was deduced that there must be a fault trending from NE to SW between GTE-7 and the geothermal manifestation area, separating the discharge area from the recharge area.

(3) Since data useful to evaluate the geothermal reservoir in the San Kampaeng was not obtained from the results of drilling at GTR-7, it was decided to perform fault and fracture detection and underground temperature survey in 1985 in and around the geothermal manifestation area to determine presence of a geothermal reservoir.

(4) Fault or fracture detection was carried out by the fingerprint geochemical survey method. From the result of survey, it was detected that there are two main faults trending from NW to SE located at the NE and SE sides of the geothermal manifestation area and other faults trending from NE to SW located north of the manifestation area.

(5) Based on he data obtained from drilling of 10 heat holes of 100 m depth and measurement of hole temperature which were carried out by EGAT, an isothermal contour line map for 100 m depth was made.

(6) The distribution map for underground temperature conforms with that of fault or fracture, and it has become clear that a high temperature zone with temperature above 70°C occupies the area surrounded by the above mentioned two faults with direction of NW-SE, and that the geothermal reservoir detected by fault and underground surveys has geometry wider than 500 m and longer than 1,000 m.

(7) Whether power generation by using geothermal steam or by the Binary Cycle System is feasible or not depends on the fluidal temperature in the reservoir. It is considered that, in

order to know such feasibility, there is no other useful way except drilling of an exploration well in the survey area.

(8) Judging from estimation of fluidal temperature by geochemical thermometer which suggests range from 160° to 200°C, and records a high underground temperature near the surface at the geothermal manifestation area of more than 100°C, drilling of an additional exploration well is warranted to study the reservoir characteristics.

(9) With regards to the site for drilling GTE-8 as planned by EGAT, it is considered that the quarry near No.9 heat hole would be suitable for the site of an exploration well.

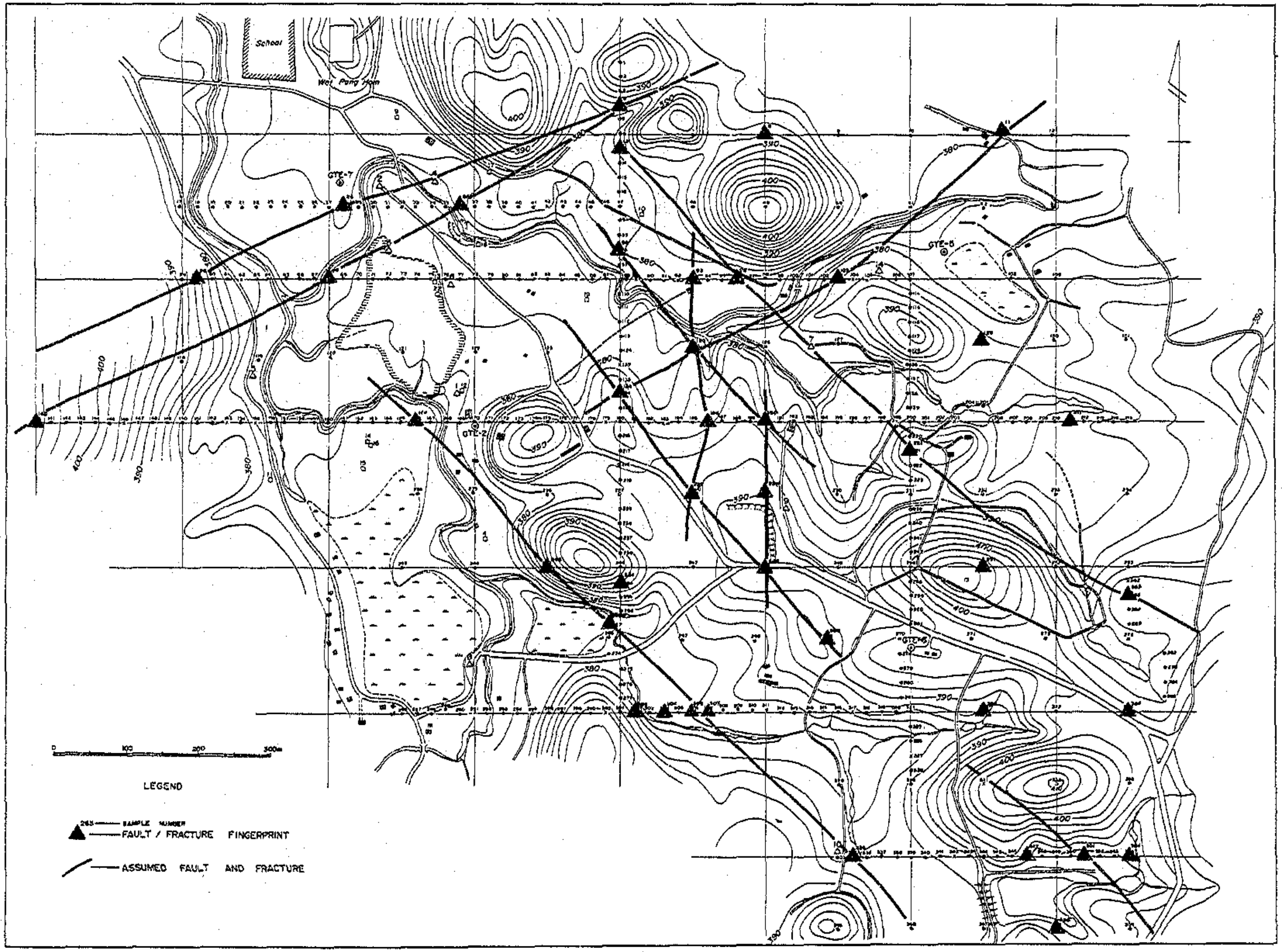

Fig. 4.2-3 Point and Pattern of Fault Fractures

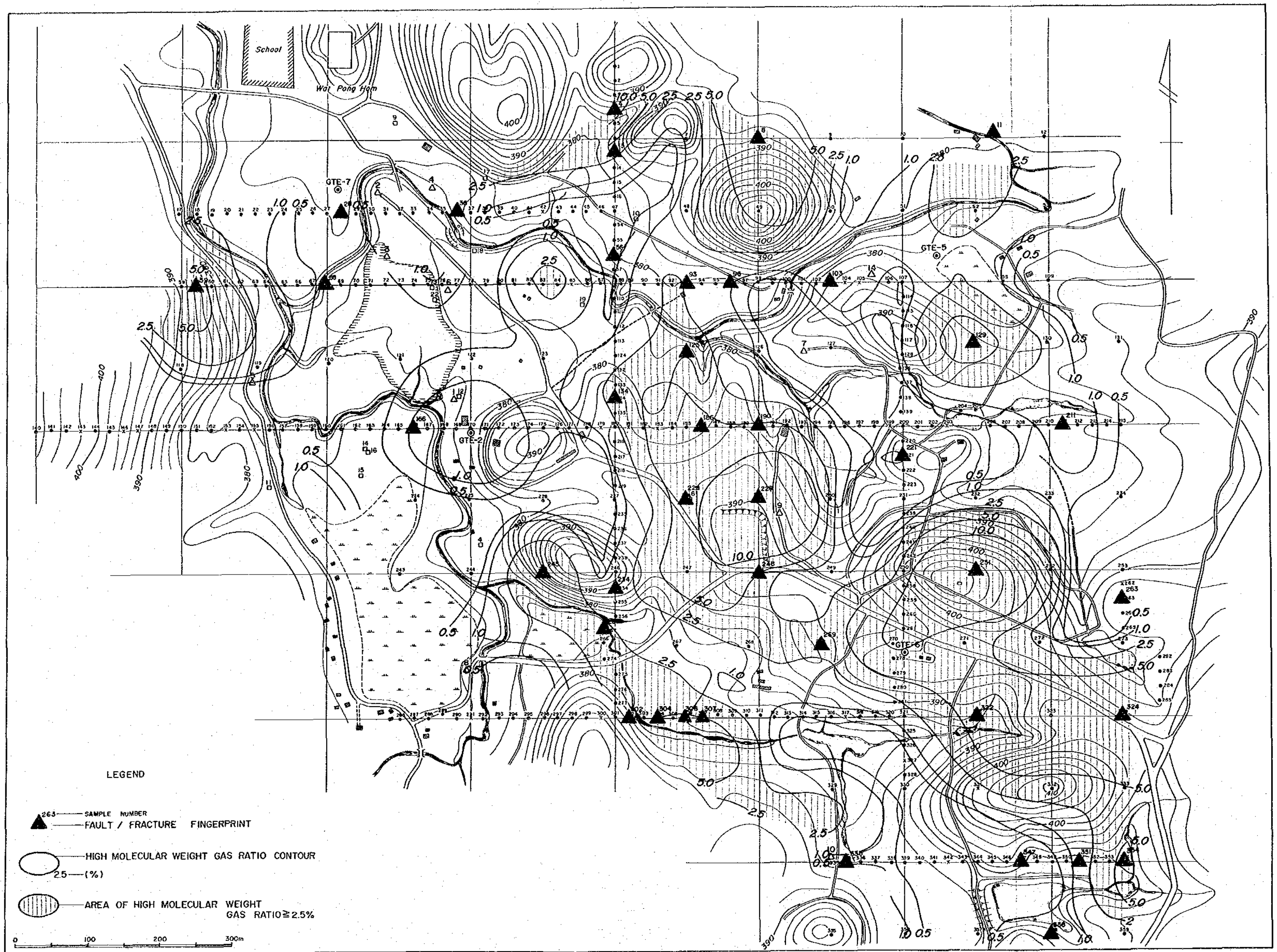

Fig. 4.2-4 Contour Map of High Molecular Weight Gas Ratio

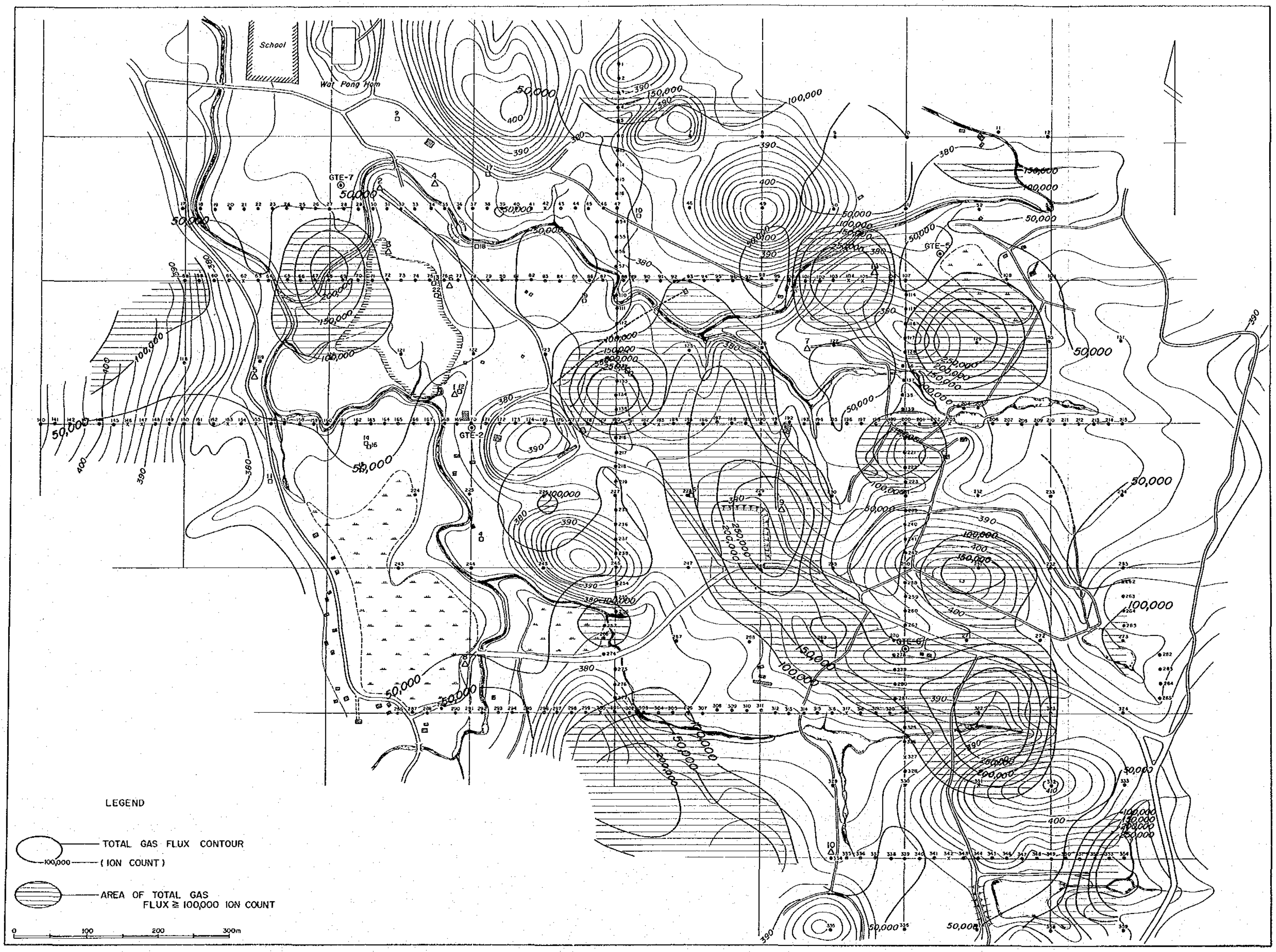

Fig. 4.2-5 Contour Map of Total Gas Flux

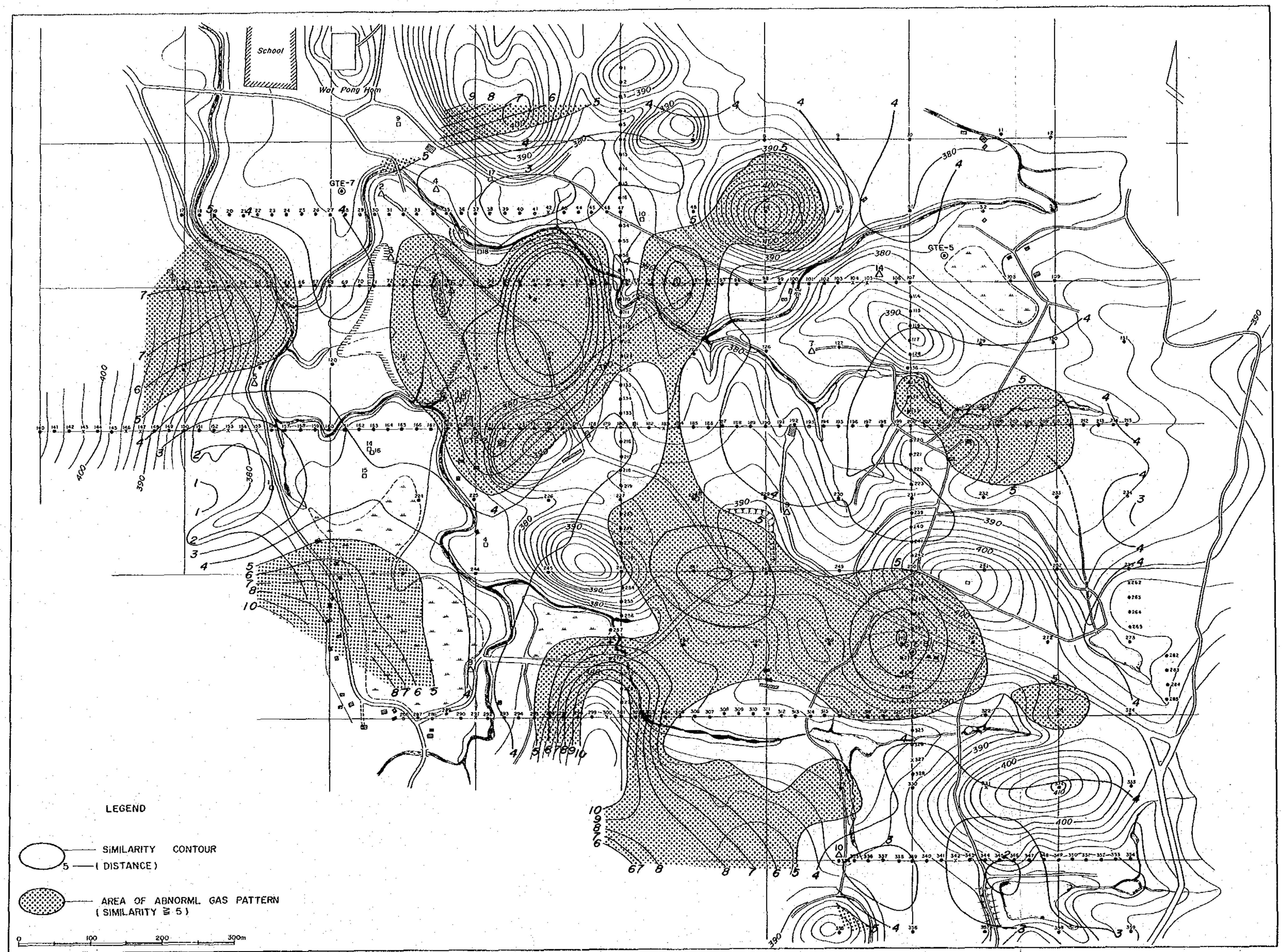

Fig. 4.2-6 Similarity Analysis

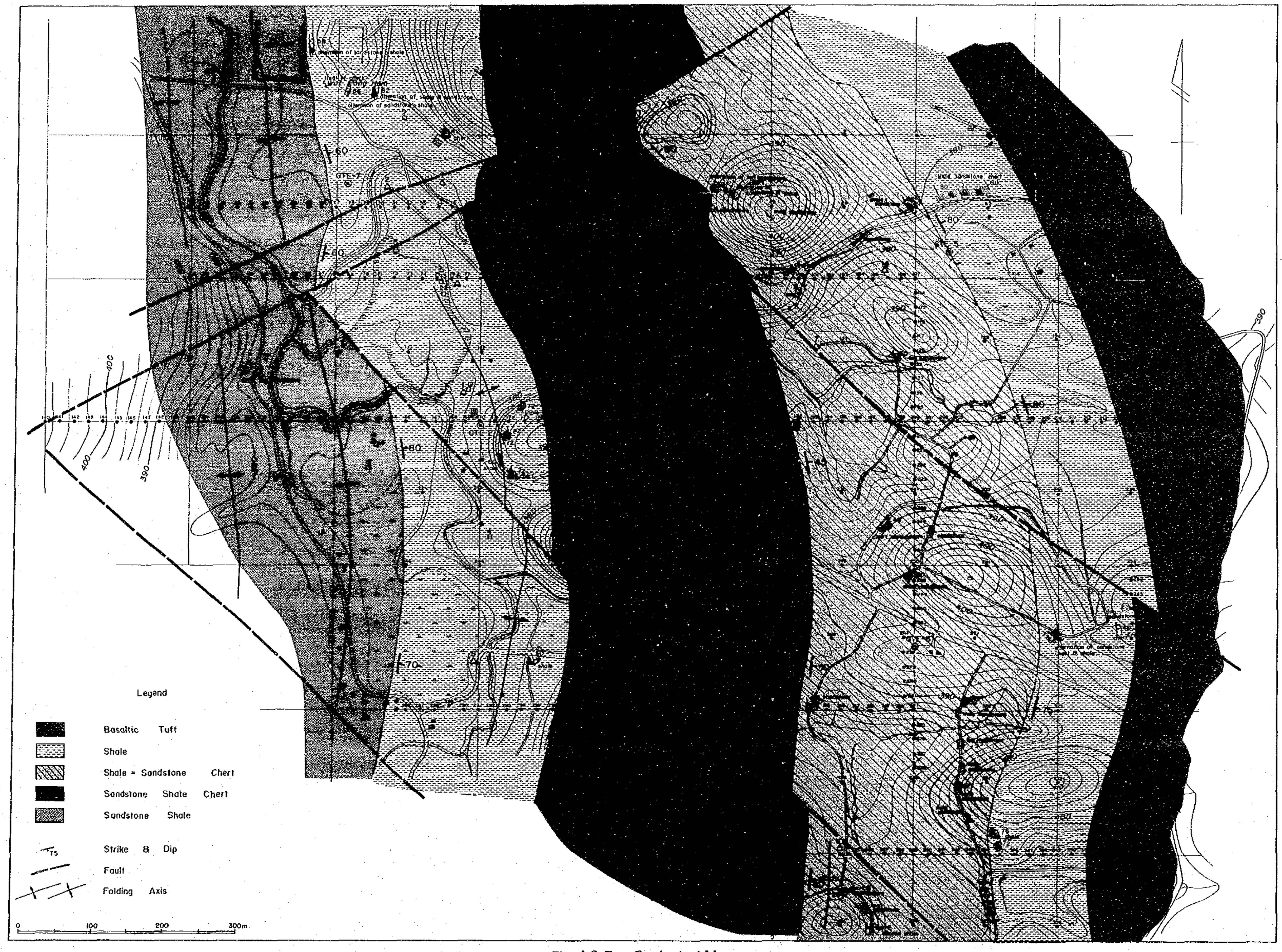

Fig. 4.2-7 Geological Map

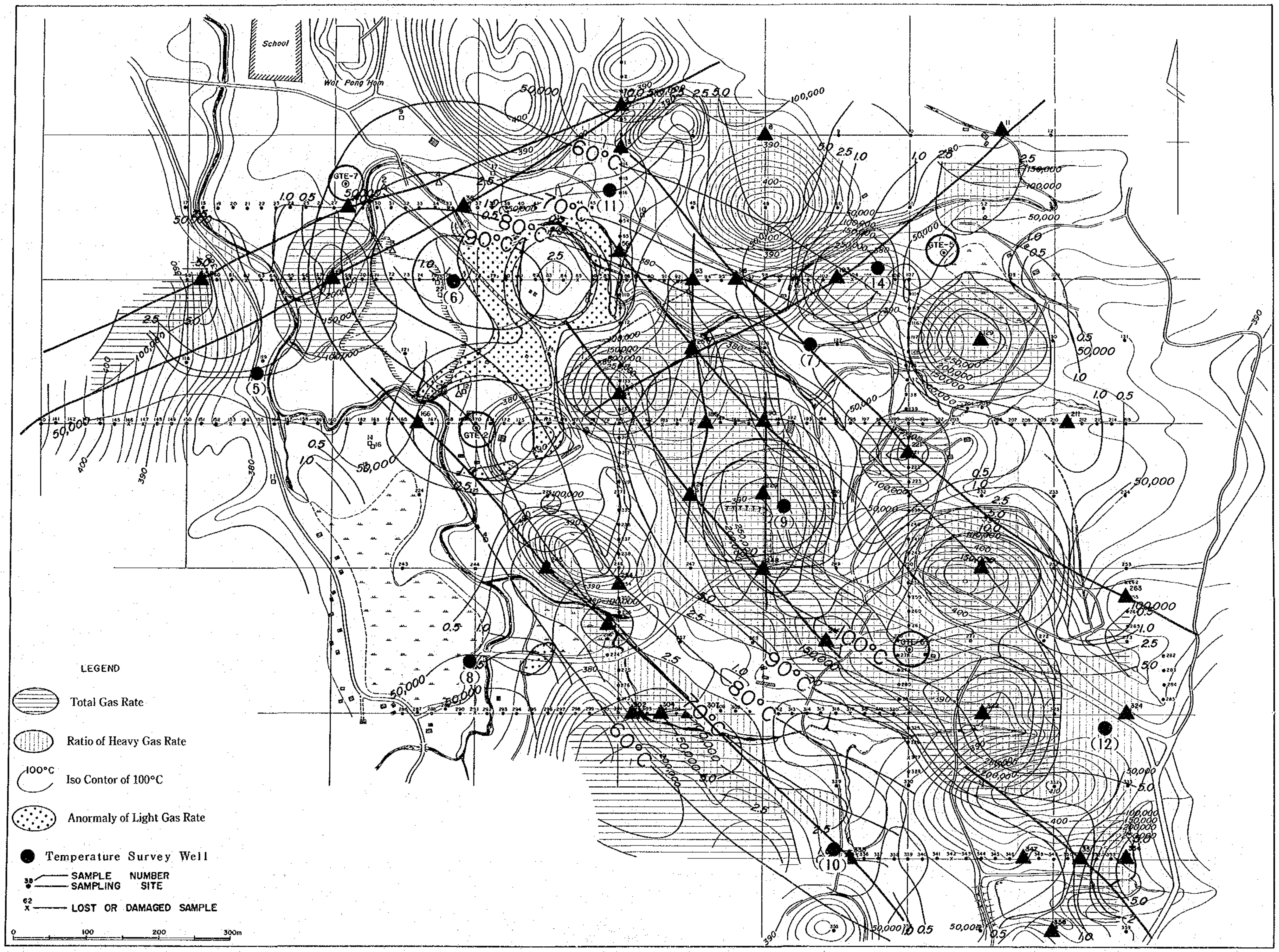

Fig. 4.2-8 Gas Concentration Anomaly

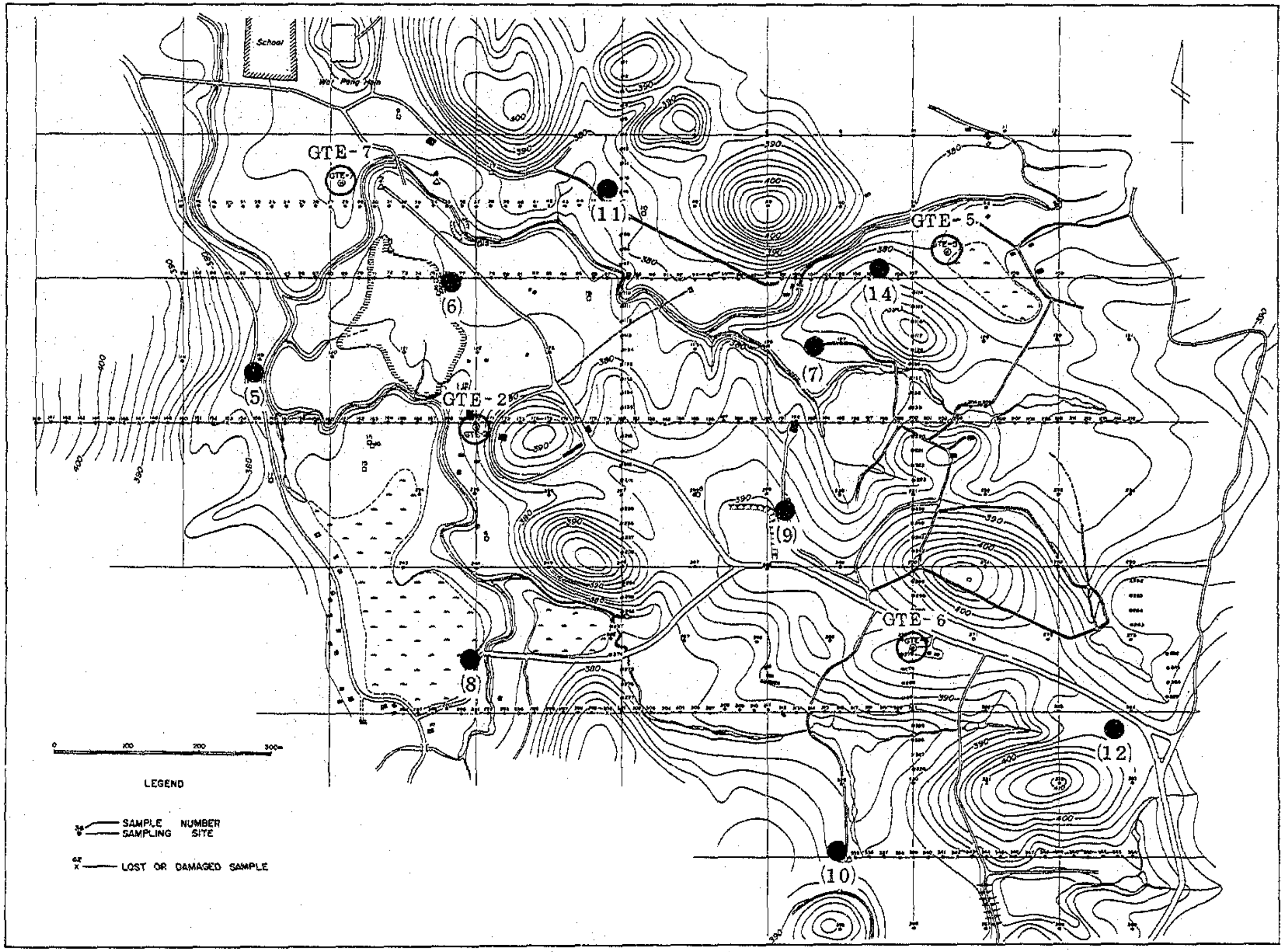

Fig. 4.3-1 Location of Temperature Survey Well

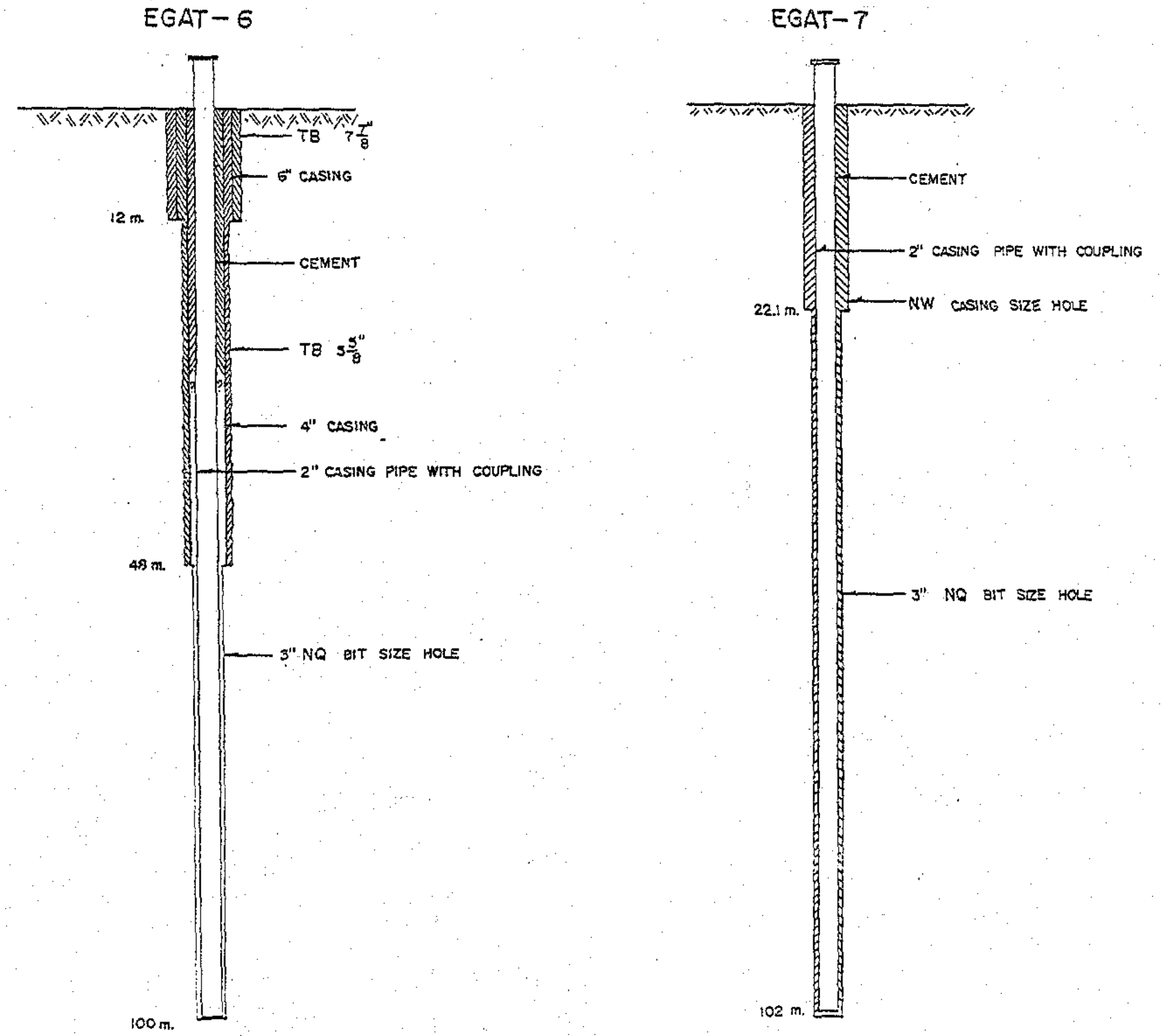

Fig. 4.3-2 Well Completion of Temperature Survery Well

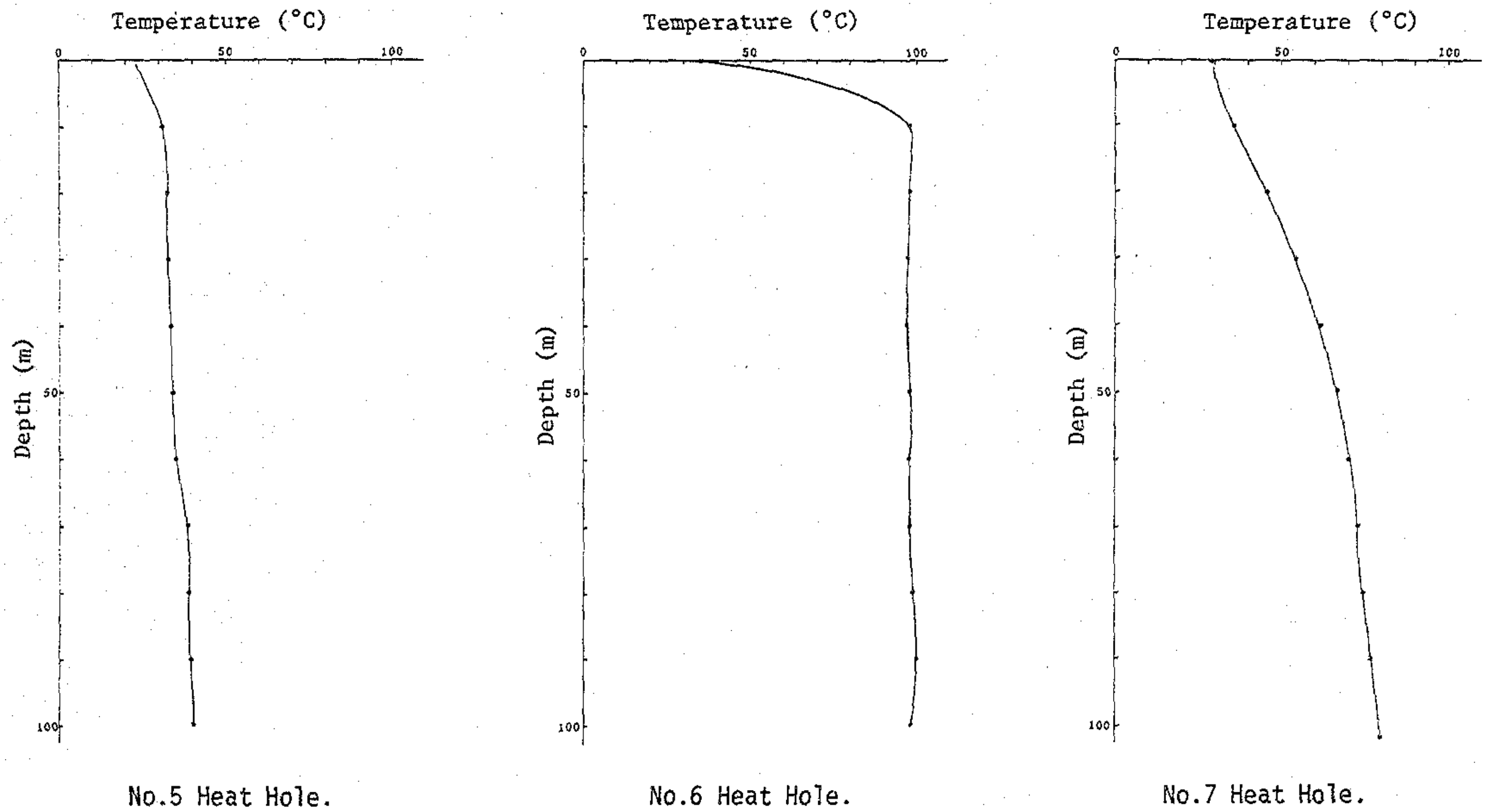

Fig. 4.3-3 Depth — Temperature Curve of Survey Well (1) ~ (3)

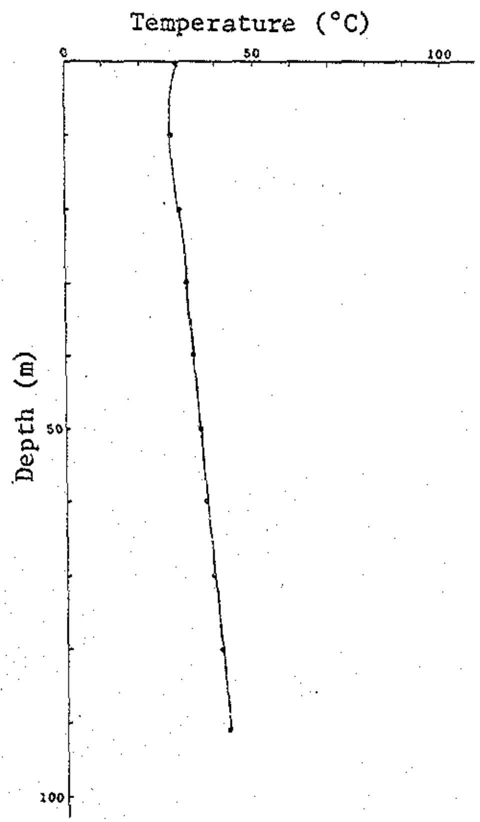

No.8 Heat Hole.

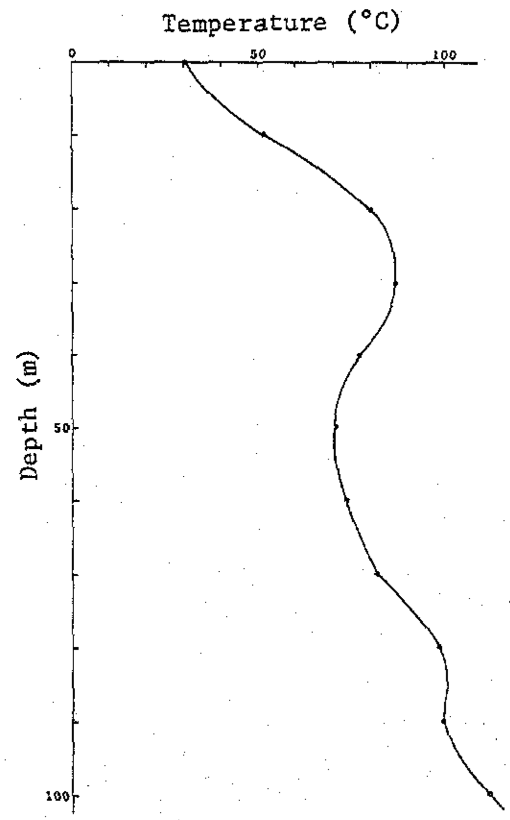

No.9 Heat Hole.

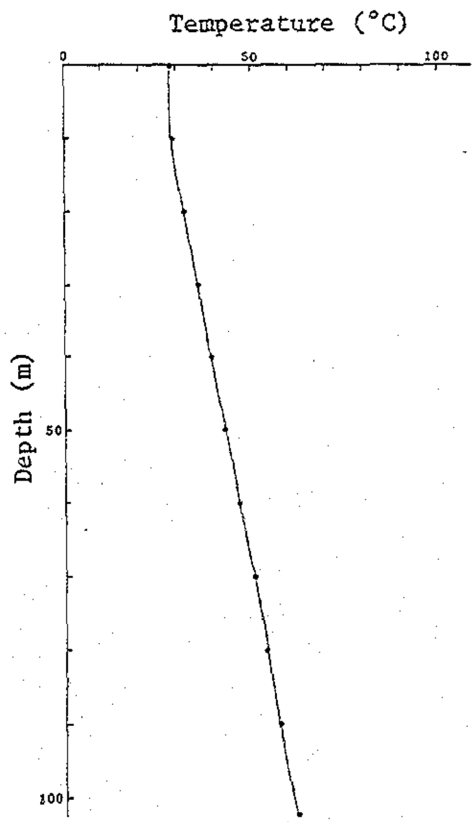

No.10 Heat Hole.

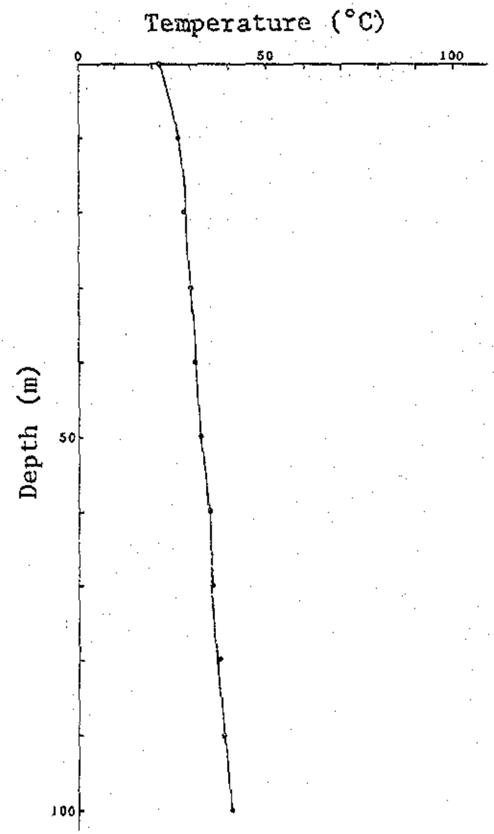

No.12 Heat Hole.

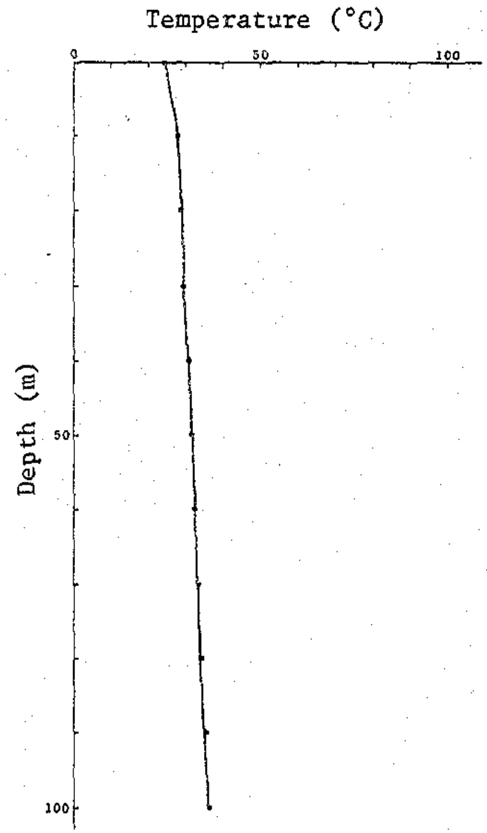

No.13 Heat Hole.

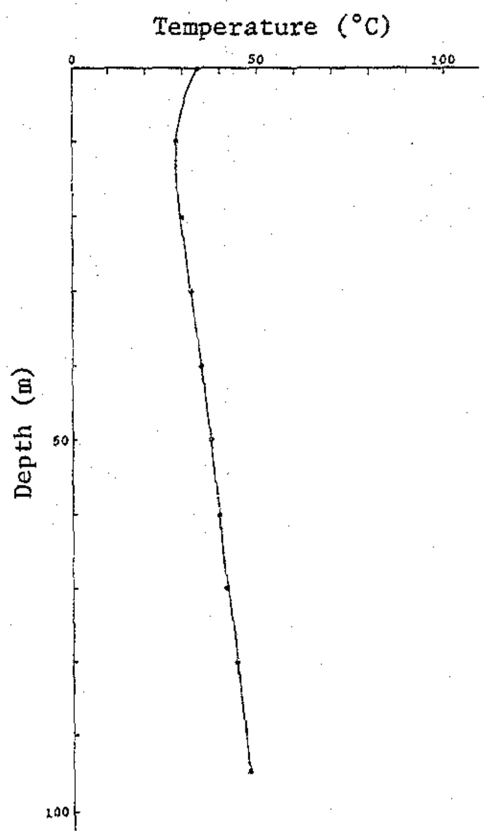

No.14 Heat Hole.

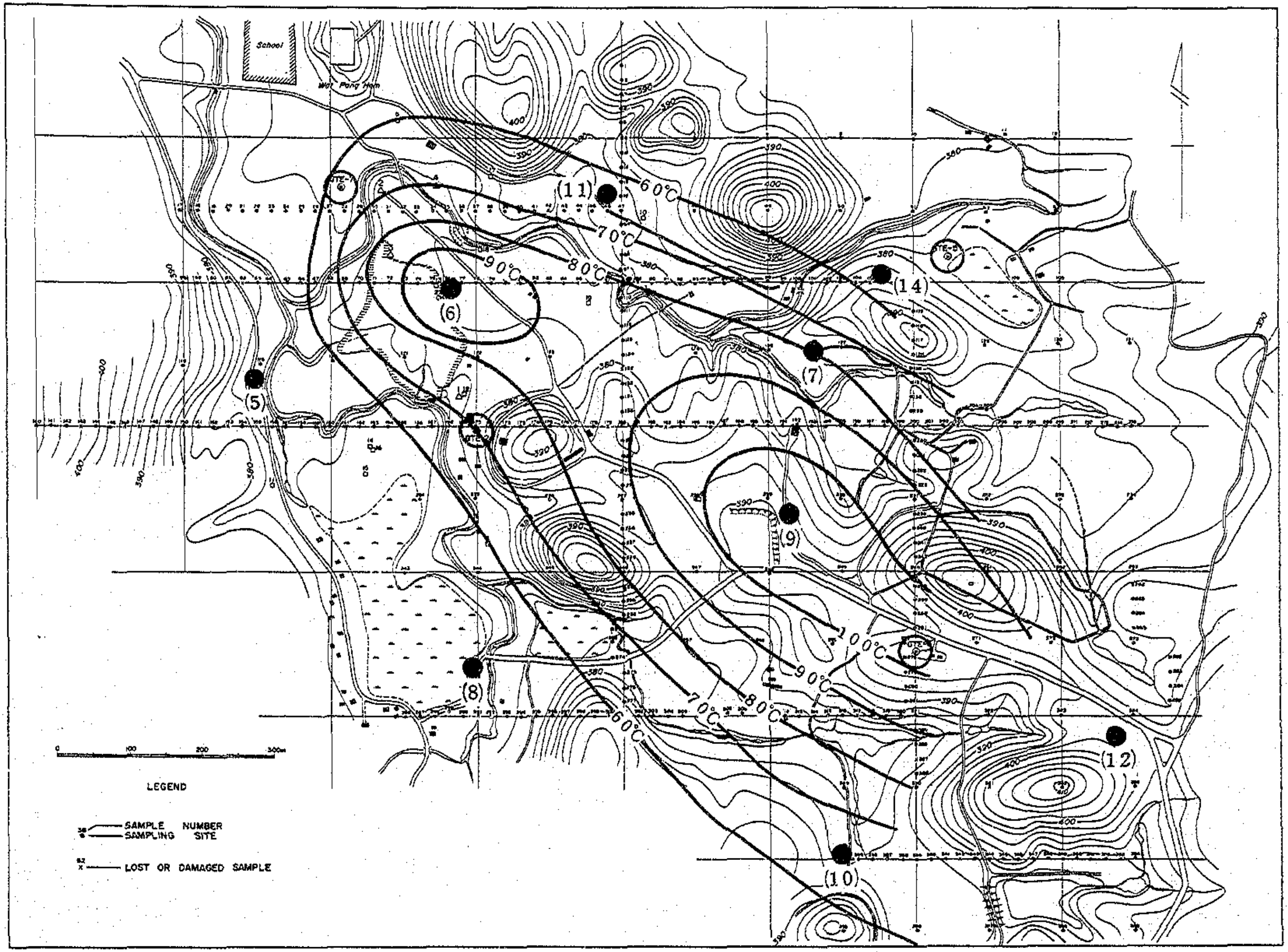

Fig. 4.3-4 Temperature Distribution at the Depth of 100 meters

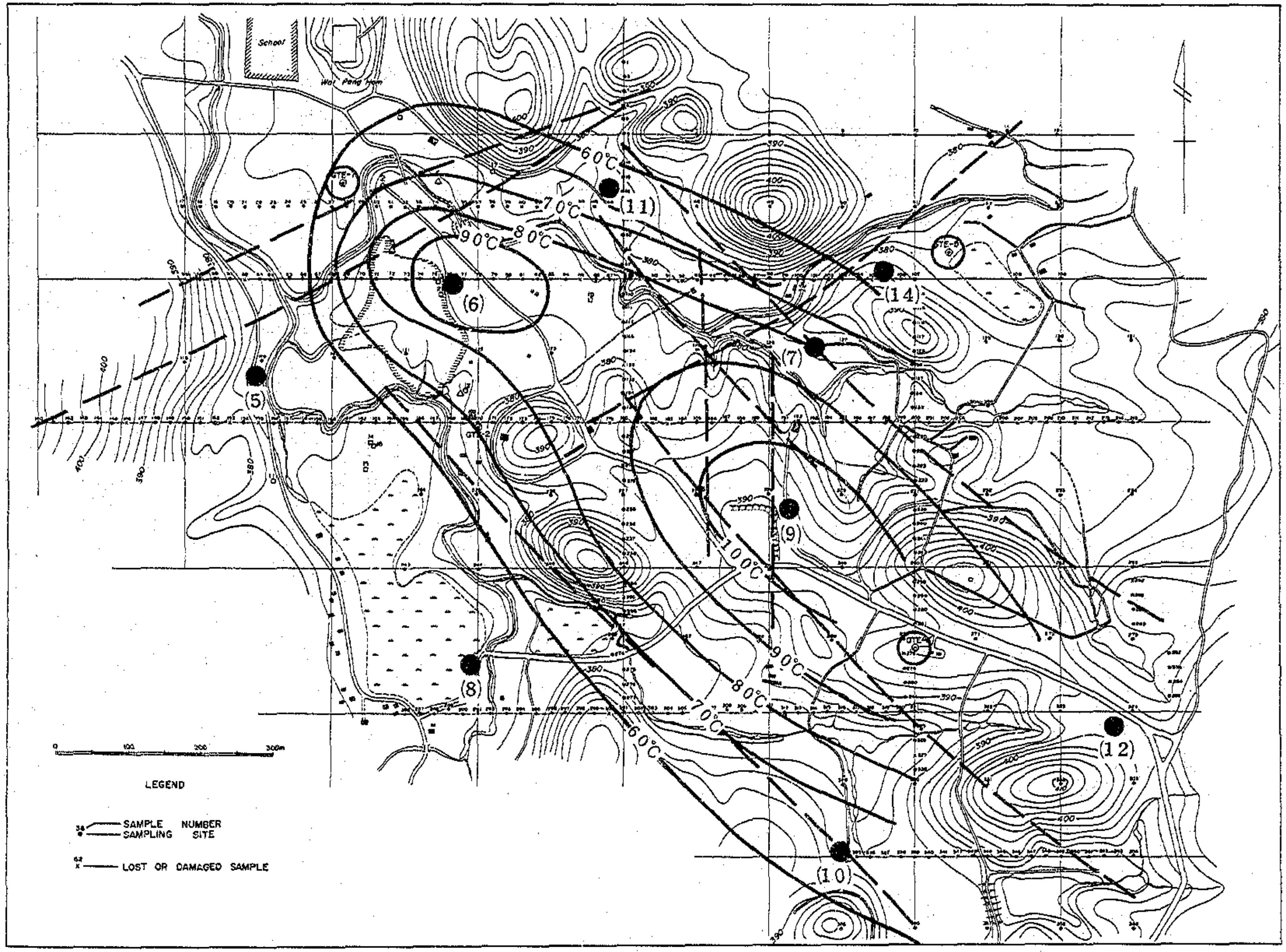

Fig. 4.3-5 Fault Structure and Temperature Pattern